

Blue wrapping paper: material properties of the recyclate and optimisation of the melting process

by

D.R. van der Heiden

to obtain the degree of Master of Science
at the Delft University of Technology,
to be defended publicly on Tuesday January 11, 2022.

Student number: 4313771
Project duration: March 1, 2021 – January 11, 2022
Thesis committee: Assistant Prof. dr. ir. T. Horeman, TU Delft, supervisor
PHD-candidate. B. van Straten, TU Delft, supervisor
Prof. dr. J. Dankelman, TU Delft

An electronic version of this thesis is available at <http://repository.tudelft.nl/>.

Abstract

Introduction

Each year hospitals in the Netherlands generate approximately 1.3 million kilogram of waste from the polypropylene (PP) wrapping paper (WP) used to wrap surgical instruments. The objective of this thesis is to acquire high quality PP, for the use of injection moulding, from blue wrapping paper waste as well as analysing and proposing solutions for optimizing the current melting process.

Method

In the first part of this thesis the WP was melted at different temperatures into bars, granulated and mixed with virgin PP. Dog bones were injection moulded to analyse the influence of the initial melting temperature, mixing ratio with virgin, pollution (sticker and tape) and ten washing cycles of disinfection at the sterilization department.

The reduction of the cycle time by means of pressure was analysed on a conceptual level. The separation of the pollution from the WP during the melting cycle with filtration was tested with three different filter designs. Finally, partitioning of the end product with a tray divider was tested.

Results

The results on the initial melting temperature show marginal differences in material properties. In general the reprocessed material behaves in a more brittle manner, with the ultimate tensile strength, Young's modulus and Shore D hardness increasing and the strain at break decreasing with amount of WP recyclate used compared to virgin material. Pollution seemed to decrease the strain at even further while also decreasing the ultimate tensile strength. The results for the washing and disinfection showed minimal material changes.

The results on the tested filtration prototypes showed that filtration can be used to separate pollution during the melting cycle. Furthermore, IR temperature measurements and flow measurements, with clean and polluted WP waste, show the importance of heat flow characteristics for an efficient filter design. The combination of a filter with proper heat flow characteristics and a conceptual pressure system showed a weight reduction of 40%. The tray divider partitioned the end product, making the end product directly implementable in a granulator.

Discussion

The changes in material properties when using 50% virgin material and 50% recyclate (50%R) indicated minimal changes when compared with 100% virgin. Moreover, this does not imply a lesser product, rather a different product. Different applications require different material properties, as such the mixing ratio can be adapted according to the applications needs.

When designing a full-scale filter it is recommended to use spikes to keep the bulk of the pollution from reaching the permeable surface of the filter. The use of a coating on a filter could reduce the time needed to clean the filter.

Conclusion

This thesis project showed that it possible to make high-quality products with the granulate obtained from blue wrapping paper waste. Also, adding; a pressure system, a filtration system and a tray divider can reduce the process time for obtaining 99% pure granulate from WP waste.

Contents

1	Introduction	1
1.1	Problem definition	1
1.1.1	Unknown material properties	2
1.1.2	Melting process	2
1.2	Objective	3
1.2.1	Mechanical material properties	3
1.2.2	Remelting process optimisation	3
2	Material properties of the recyclate	5
2.1	Method	5
2.1.1	Remelting and granulating of WP waste	5
2.1.2	Injection moulding	5
2.1.3	Influence of pollution on the properties of reprocessed WP waste	5
2.1.4	Material properties of reprocessed WP waste and mixed with virgin	6
2.1.5	Analysis	6
2.1.6	New products made from WP for the sterilisation department	6
2.2	Results	7
2.2.1	Melting and granulating	7
2.2.2	Influence of the melting temperature on reprocessed WP waste	7
2.2.3	Influence of the mixing ratio	8
2.2.4	Influence of stickers and tape on the properties of reprocessed WP waste	8
2.2.5	Influence of ten cycles of washing & disinfection	9
3	Remelting process optimisation	11
3.1	Method	11
3.1.1	Global process optimisation	11
3.1.2	Decrease process time	12
3.1.3	Pollution separation	13
3.1.4	Improved end product	14
3.1.5	Conceptualisation	15
3.1.6	Conceptual evaluation	18
3.1.7	Tests for evaluation	19
3.2	Results	23
3.2.1	Prototypes	23
3.2.2	Test results	24
3.2.3	Reevaluation	27
4	Discussion	29
4.1	Material properties of the recyclate	29
4.2	Remelting process optimisation	29
4.3	Recommendations & limitations	30
5	Conclusion	33
A	Matlab code: material properties	35
B	Linear fit of the material properties with a 95% prediction interval	39
C	Matlab code: Temperature profile	43
D	FEM analyses: stress strain figures	47

Introduction

It has been calculated that 275.000.000 tons of plastic waste was generated in 2010, in 192 coastal countries alone (Hoegh-Guldberg, 2015). Unfortunately, hospitals are no exception to the rule. With the volume of medical waste growing over the years (Razali and Ishak, 2010; Manga et al., 2011; Haque et al., 2021). Moreover, the amount of waste produced by the hospitals has increased another 30% during the COVID-19 pandemic (Silva et al., 2021; Sutrisno and Meilasari, 2020). Hospitals in the Netherlands contribute around 7% to the total CO_2 -eq emission and around 7%-10% to the total CO_2 -eq emission in the US (Strategists, 2019; White et al., 2010; Eckelman and Sherman, 2016).

In the Netherlands it is common practice to classify all waste from the operating room (OR) as regulated medical waste (RMW). Because of this classification it is incinerated. Not only does incineration of the waste have a negative effect on the environment, but the disposal through incineration is also associated with health risks (Bokhoree, 2014; Zhang et al., 2013; Yong et al., 2009; Assemu et al., 2020; Irianti, 2013; Silva et al., 2021). This has not gone unnoticed, with the public expressing increasing concerns, regarding the disposal of the waste (Pullishery et al., 2016; Chudasama, 2014; Pinto et al., 2014; Ghodrat et al., 2017). The OR is estimated to produce between 20% and 30% of the total hospital waste (Goldberg et al., 1996; Lee and Mears, 2012; Penn et al., 2012). By separating waste in the OR some of the waste can be diverted from incineration. This does not only have the obvious environmental and health benefits, but separation can also reduce costs for hospitals (Shum et al., 2020; Babu et al., 2019; Rigante et al., 2017; Bliss et al., 1995; Southorn et al., 2013; Wyssusek et al., 2016). The disposal of RMW can be 10 to 20 times more expensive than regular waste (Shum et al., 2020). To reduce the pollution and costs of the OR, recycling would be a logical next step.

Polypropylene (PP) WP is used in every surgical procedure, as such it a large contributor to the waste production from the OR; PP WP accounts for 16%-20% of the waste from the OR (McGain et al., 2015; Babu et al., 2019). Moreover, the WP is not contaminated, as it would otherwise be classified as RMW. Wrapping paper is used to wrap an instrument tray with surgical instruments. The WP forms a barrier around the tray, allowing the instruments to remain sterile. The barrier is important to prevent cross-contamination in the OR department. To further reduce chances of cross-contamination virgin material is used for the WP, meaning the material has never been used before.

Earlier studies reported the possibility of the recycling of WP to reduce waste disposal costs (Babu et al., 2019; Voudrias, 2018). However, these studies do not show concrete solutions for reusing the recycled material as products in the hospitals. A good solution to the vast amounts of WP waste could be a local circular material loop. In such a loop the hospitals become the supplier of the raw material that is needed to make the products they use themselves. When designing new products (for the hospital) with recycled material, it is important to know the material properties. With this knowledge it is possible to adapt the design such that it fulfils the products criteria.

1.1. Problem definition

To tackle the problem of the large PP waste stream, two sub-problems are analysed and discussed below. Firstly, the material changes of PP associated with the remelting and injection moulding process. Secondly, the current remelting process for large amounts of WP waste and its limitations.

1.1.1. Unknown material properties

During recycling the material properties of PP change due to chain scission and an increase in crystallinity (Aurrekoetxea et al., 2001; da Costa et al., 2007; Hyie et al., 2020). This change can be attributed more to high shear levels than to the high temperatures (da Costa et al., 2007). The Young's modulus and ultimate tensile strength (UTS) decrease only slightly, whereas elongation at break and impact strength decrease rapidly with the increase of recycling steps (da Costa et al., 2007; Hyie et al., 2020). There are also studies that show the Young's Modulus and UYS increasing with the number of recycling steps (Aurrekoetxea et al., 2001). Another important parameter of the process is the injection temperature. This temperature has the most significant negative effect on the stress at break and energy to break (da Costa et al., 2007). The general consensus is that PP becomes more brittle with an increase of recycling steps (Hyie et al., 2020; Aurrekoetxea et al., 2001; da Costa et al., 2007; Gabriel and Tiana, 2020). The change of the material can be reduced by adding virgin material to the recycled PP (Gabriel and Tiana, 2020). To the writers knowledge, no studies were found on the material properties of recycled PP from WP waste.

1.1.2. Melting process

The current process for remelting large amounts (21 kg, per cycle) of WP waste is with the Sterimelt, see figure 1.1. The Sterimelt is a large oven developed by TCG solutions and is currently used by Greencycle. Unfortunately, the Sterimelt has multiple limitations, which will be shortly discussed below.

Product pollution Figure 1.2 shows the end product of the Sterimelt. The end product is polluted with tape and partly unmolten. This tape is used to ensure that the WP stays around the sterile instrument net. Other pollution include: stickers, needles and paper sheets. TCG recommends the user to manually remove tape and other pollution, which is a labour intensive process.

Complex end product Due to the shape of the melting plates, see figure 1.1, part of the material comes out unmolten, see figure 1.2. The unmolten plastic can clog up the granulator and is unfit for the injection moulding machine. Furthermore, the length of the end product is 880mm long, 250mm wide and about 120mm high. This makes the end product too large for an average sized granulator.

Process time The heating plates reach a temperature of about 360° C. The time needed to (not fully) melt 21 kg of PP is disproportionate with the set temperature. The sheets are filled with air, it is assumed this air works as an insulator mainly against convective heat. To overcome this, direct contact with a hot surface is needed (e.g. conduction). As of now the Sterimelt relies on the weight of the waste for contact with heating plates.



Figure 1.1: The Sterimelt, oven currently used for remelting large amounts of WP waste. Left: The inclined heating plates on which most of the plastic melts. Right: Complex shape of the loading bay of the Sterimelt.

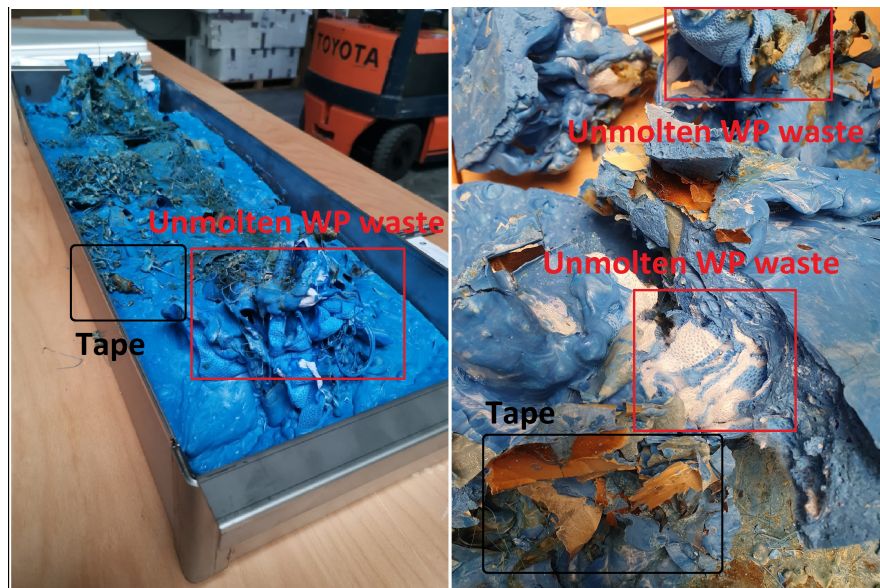


Figure 1.2: Tape and unmolten material in the end product of the Sterimelt.

1.2. Objective

The objective of this thesis is to acquire high quality PP, for the use of injection moulding, from blue wrapping paper waste as well as analysing and proposing solutions for optimizing the current melting process. To do this, two separate analyses are conducted. Firstly, the material properties of the WP after remelting and injection moulding will be analysed. The material properties are analysed first to see if the recycled material can be used. Secondly, the current melting process with the Sterimelt will be analysed and concepts are made to improve the remelting process.

1.2.1. Mechanical material properties

During my internship the material properties of the remolten plastic without injection moulding were analysed (van der Heiden, 2020). Unfortunately, the material properties of the remolten plastic were insufficient due to the inhomogeneous end product. Therefore, the remolten product will be granulated into granulate and used as raw material for injection moulding. To explore the effects of different variables on the material properties of PP WP waste during the remelting process three research questions are made.

1. Does the melting temperature influence the mechanical properties of reprocessed WP waste material?
2. Does mixing of virgin and recycled PP alter the mechanical properties?
3. Does commonly seen pollution, debris from stickers and tape, influence the properties of the reprocessed WP waste?

1.2.2. Remelting process optimisation

The goal of the process optimisation is to minimize the time to make 99% pure PP granulate from WP waste. To do this the remelting process is analysed and different solutions are explored. To give structure to the process optimisation, the goal is split up in three sub-goals.

1. Minimize the cycle time during the melting process.
2. Separate pollution from the wrapping paper waste.
3. Breaking up the end product for granulation.

2

Material properties of the recyclate

This chapter presents the method for the remelting process of the recycled PP used for mechanical tests and the method for the mechanical tests. Moreover, the results on the mechanical properties of the recycled WP waste are presented¹.

2.1. Method

First, the remelting method is presented. Second, the process of granulating and injection moulding of the remelted product. Third, the method for obtaining different mixing ratios and polluted materials is presented. Finally, the method for collecting and analysing the data from the injection moulded product is elaborated.

2.1.1. Remelting and granulating of WP waste

The WP waste was manually placed into a tubular cylinder with a diameter of 100 mm, closed on each side, and placed in an electrical melting oven (KOS, Electric crucible, series 219029). The top of the cylinder has a piston with a spring system, this maintains pressure during the melting which reduces the melting time, see figure 2.1. The remelted bars were granulated using a Moditec grinding mill Gplus 2 and directly injection moulded at 200°C. To determine the influence of the melting temperature of the WP waste, the WP was first melted at 200°C, 250°C and 300°C. Pictures of various stages of the remelting process can be found in figure 2.1. The melting temperature with the most favourable properties is evaluated and used to melt the next batches. Virgin granulate is mixed before injection moulding with recycled PP (ratio indicated as %R).

2.1.2. Injection moulding

Two different moulds were manufactured and used for injection moulding (Babyplast, injection moulding machine 6/10P). One with a dog bone design that is used for tensile testing, as shown in 2.2, to make dog bones of different qualities (Supplementary File 1). The second mould was made for an instrument opener, having the form of a cross. The purpose of the medical device is to keep double hinged instruments open during washing and disinfection at the Central Sterilisation and Services Department (CSSD). It is important to keep instruments in an open position during washing so that all parts of the instruments are properly cleaned in the CSSD.

2.1.3. Influence of pollution on the properties of reprocessed WP waste

Paper, tape, and stickers can end up in the WP recycling process and pollute the PP end product, see figure 1.2. This pollution could not only affect the material properties but could also clog or damage injection moulding machines. A worst-case scenario was therefore included in the tests in which the concentrated residual material was removed from the filter after an unsorted batch of WP waste had been processed in the melting furnace. This residual material, which consisted of around 50% pollution, was granulated, and used to produce five worst-case scenario samples.

¹The method and results presented in this chapter are the basis for the publication van Straten et al., 2021.



Figure 2.1: Overview of the remelting stages. From top left to bottom right: Collected WP waste, Melted WP into bars, Spring loaded system, Granulate, Filter in melting cylinder, Residue removed from filter and used for polluted dog-bones.

2.1.4. Material properties of reprocessed WP waste and mixed with virgin

For analysis and to compare strengths, six different sets of five dog bones each were made from PP, melted at the most favourable temperature and injection moulded at 200°C in different mixing ratios. Six sets of at least five dog bones in various mixing ratios:

1. 100% virgin PP used as benchmark (Virgin).
2. 25% recycled mixed PP WP with 75% virgin PP (25%R).
3. 50% recycled mixed PP WP with 50% virgin PP (50%R).
4. 75% recycled mixed PP WP with 25% virgin PP (75%R).
5. 100% recycled PP WP(100%R).
6. 100% recycled PP WP, polluted with stickers and tape (Polluted).

The melting and injection moulding parameters used for the collected PP WP can be found in supplementary file 2.

2.1.5. Analysis

A tensile strength test was carried out to analyze the mechanical properties of the PP dog bones. Material degradation is accelerated if the PP waste contains pollution such as tapes and stickers or if PP is mixed with other types of plastic (Hyie et al., 2020). The Youngs modulus, E , is assessed by measuring the elastic behaviour (ratio of stress to axial strain - $E = \sigma/\epsilon$) over the first 1% elongation, as is common practice for plastics. The ductility of the material is analysed by measuring the elongation at break as a percentage between the changed length and the initial length after the dog's bones had broken. The ultimate tensile strength (UTS) is measured to indicate the maximum tensile stress of the material and Shore D to measure the hardness of the dog bones. The Matlab® code used for the data processing of the dog-bones can be found in appendix A. The dog bones are compared in combined stress-strain relationship measured with a tension bench (Delft University of Technology, Faculty of Mechanical Engineering, Zwick Roell, Zwick GmbH & Co.KG, Ulm, Germany), as shown in figure 2.2. The dog bones have a shoulder on either end. The shoulders ensure no slip occurs while testing. Furthermore, the dog bones were tested with a Shore durometer (Sauter, HBD 100-0.HBD 100-0, Durometer, www.sauter.eu) to measure the hardness of the dog bones.

2.1.6. New products made from WP for the sterilisation department

To verify that products made of recycled WP can withstand the washing cycle at the CSSD, extra tests were conducted. To determine the influence of the washing cycles on the material properties of recycled

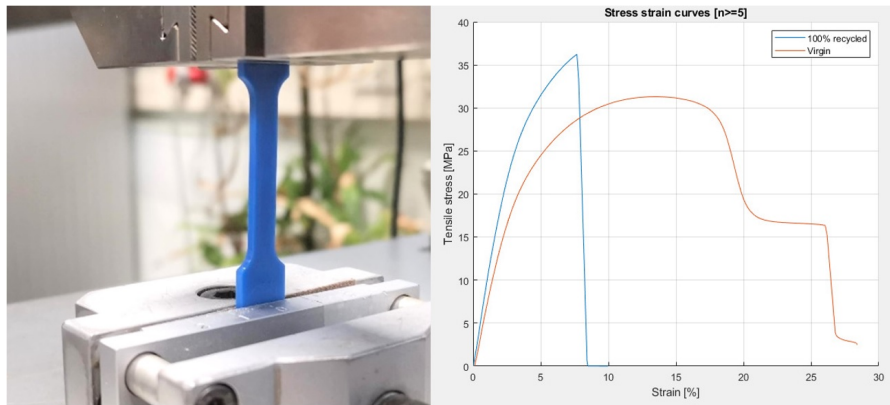


Figure 2.2: Tensile test. Left, dog-bone in the clamps of the tensile testing machine. Right, Example of stress strain curves of virgin and 100%R.

PP dog bones were made from virgin, 50%R, and 100%R. The dog bones were tested before and after ten washing cycles in a Getinge G1-WA-04, thermal disinfecter (Getinge. Lindholmospiren 7, SE-417 56 Gothenburg, Sweden) at the CSSD Services. With the insights gained from these tests an instrument opener was designed for double hinged instruments.

2.2. Results

In this chapter results are presented on the material properties.

2.2.1. Melting and granulating

After melting, the cylinders were emptied with melted PP bars as a result. The bars were granulated into granulate, the raw material for injection moulding. At the top of Figure 2.4 pictures of the dog-bones that were injection moulded with different mixing ratios can be found. For clarification, the structure of the polluted dog-bone (right in figure 2.4) was enlarged 5x and the contrast was enhanced to better expose the particles.

2.2.2. Influence of the melting temperature on reprocessed WP waste

Throughout the injection moulding process all mixes flowed smoothly, according to Pieter van Nimwegen from Model Engineering, an injection moulding expert. No other problems were detected during the injection moulding of dog bones or instrument openers, with any of the mixes. The tensile test results for the melting temperature can be found in Figure 2.3. From left to right: Dog-bones made from 100% recycled WP melted at 200°C, 250°C and 300°C. No significant differences were found between the dog

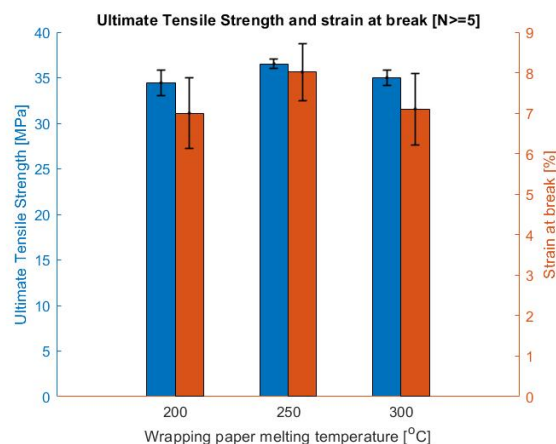


Figure 2.3: Ultimate tensile strength and strain at break made from 100% reprocessed WP remelted at different temperatures.

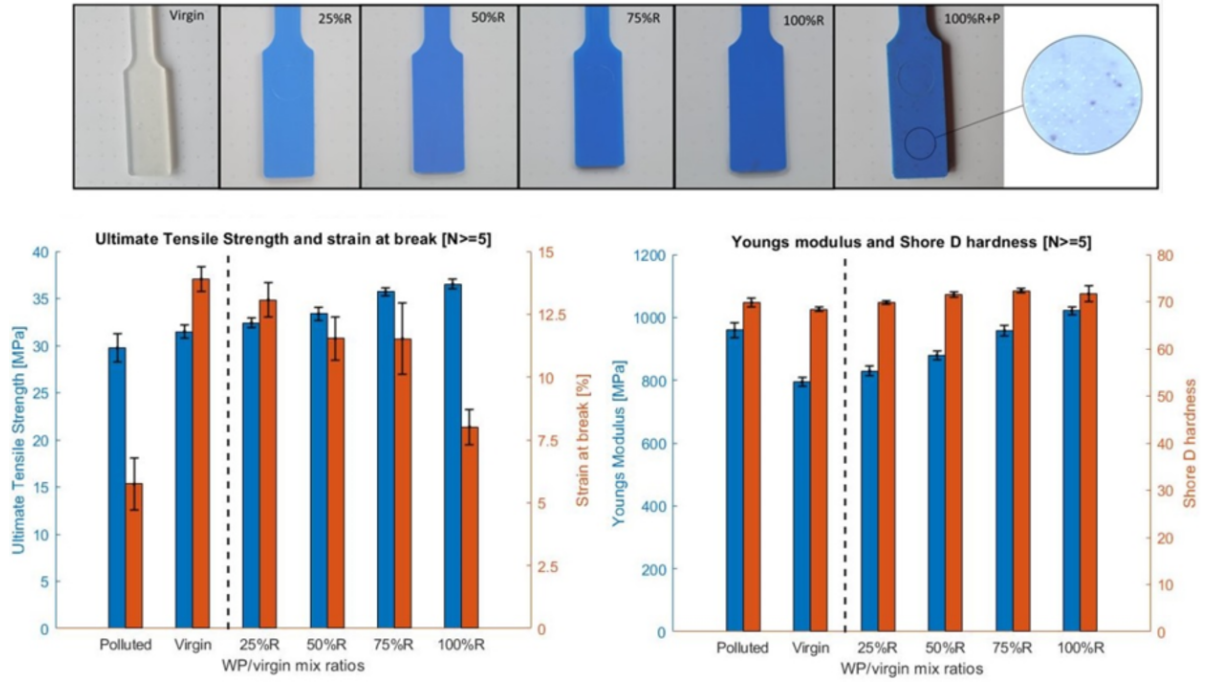


Figure 2.4: Dog-bones and their material properties. Top, Pictures of different dog-bones. Bottom left, Ultimate tensile stress and strain at break. Bottom right, Youngs modulus and hardness in shore D.

bones made from remelted WP at different remelting temperatures. As the remelting temperature of 250°C seemed to give the most favourable results, all subsequent tests were made with the granulate from remelted WP at 250°C .

2.2.3. Influence of the mixing ratio

Figure 2.4 shows the results for the polluted scenario, virgin PP, and different mix ratios. The Ultimate Tensile Strength (UTS) appears to be, apart from the polluted dog bone, above 30 MPa. The UTS increases from 31.5 MPa with Virgin to 36.5 MPa for 100%R. The dog bones made from 100%R granulate show an approximately 6% lower strain at break than Virgin PP. The results show that mixing recycled PP with virgin PP increases the strain at break, depending on the mixing ratio, with a maximum of 5%. Figure 2.4 right shows the material hardness, measured in Shore D values in combination with the Youngs modulus. The bars indicate that the tensile stiffness and hardness increase as the amount of recyclate in the mix increases. Finally, a first-degree polynomial was fitted through the average of the material properties, see formulas 2.1 to 2.4 below. Here x is the percentage of virgin material used.

$$E = 2.32 * x + 780 \quad (2.1)$$

$$\sigma_{UTS} = 0.05 * x + 31.2 \quad (2.2)$$

$$\epsilon_{break} = -0.05x + 14.3 \quad (2.3)$$

$$ShoreD = 0.036 * x + 68.9 \quad (2.4)$$

The graphs of the linear fit with the 95% prediction interval can be found in appendix B.

2.2.4. Influence of stickers and tape on the properties of reprocessed WP waste

The tensile tests conducted on the dog bones which were injection moulded with pollution in the granulate, as a worst-case scenario, showed a strain of 6% (SD1) and UTS of 29.8 (SD1.4) MPa. Both the polluted and 100%R dog bones show similar tensile stiffness and hardness. However, the UTS and the strain at break differ significantly between the polluted and the 100%R dog bones.

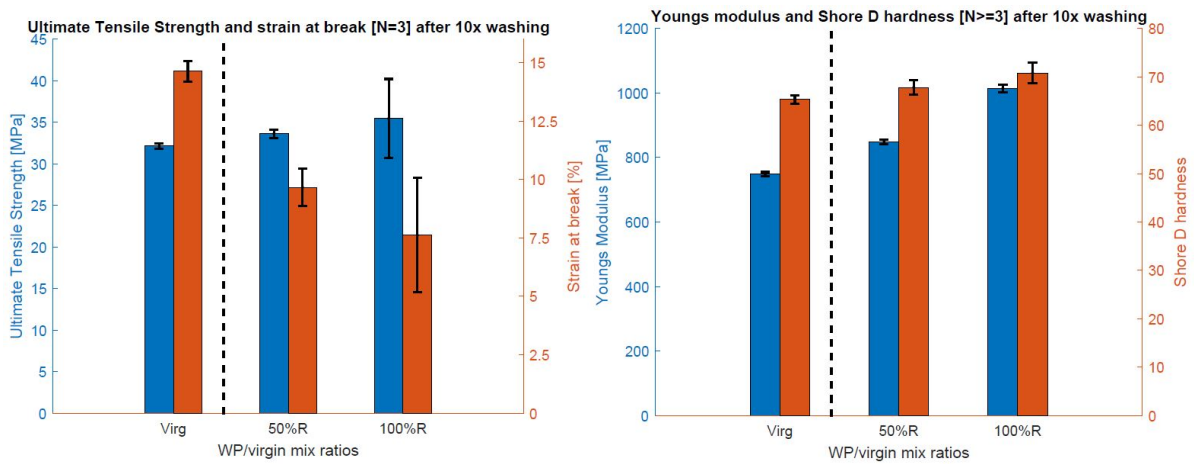


Figure 2.5: The Ultimate Tensile Strength, strain at break, Youngs modulus and hardness after 10 cleaning and disinfection cycles.

2.2.5. Influence of ten cycles of washing & disinfection

The results of the tensile and Shore tests of the dog bones made of virgin, 50%R and 100%R that were washed for ten cycles in the CSSD (Supplemental File 3) are presented in figure 2.5. The changes to the material properties were minimal compared to the results as presented in figure 2.4.

3

Remelting process optimisation

In chapter 2 the melting tube used for acquiring recycled granulate had a filter and a pressure system. The filter separated the pollution and the spring loaded piston decreased the melting time, see figure 2.1. Both separation of the pollution by means of filtration and pressure during the melting process to decrease time showed promising results. With the knowledge on the remelting process from the previous chapter the current remelting process is analysed in this chapter. Firstly, the method for analysing, finding solutions, conceptualising and evaluating these concepts for the current remelting process is elaborated. After which, the prototypes are dimensioned and the results of the tests are presented. Finally the concepts are reevaluated with knowledge gained from the tests.

3.1. Method

The main objectives of the solutions are to minimise the time to melt WP waste, separate the pollution and to reduce the complexity of the end product. The process is first analysed on a global level. Subsequently, global solution methods are analysed in more detail. After which, concepts are made and evaluated. Finally, tests are elaborated to test certain criteria of the concepts.

3.1.1. Global process optimisation

The global solution method with a corresponding explanation, for the design goals of the current melting process can be found in the figure 3.1. The solutions in red will not be further explored as these are not achievable with a new concept. The solutions highlighted in green are solutions that will be explored in the subsequent subsections.

Legend					
Design goals					
Global solution method					
Decrease processing time	Temperature increase	Pressure increase	Melting zone increase	Volume increase	
	Increase temperature for faster melting Limit: 380° C: spontaneous combustion ¹	More pressure on waste: increases the amount of PP in contact with the heating plates	Increase the area where melting of the PP occurs	Larger Sterimelts More Sterimelts	
Pollution separation	Before melting	During melting	After melting		
	Remove stickers and tape before the melting process	Separation of the pollution while the PP is liquid	Removing the pollution from the end product		
Improved end product	Partitioning of the end product		Pelletizing during melting		
	Break up the end product such that it can be implemented into an average sized granulator		Pelletize the PP while it is liquid		

Figure 3.1: Process optimisation global overview. Red: Not achievable with a new concept or requires existing solution. Green: Needs further exploration. [1] = C, 2020.

After the analyses of the global solution methods, the solutions will be substituted into figure 3.1. This will result in one large morphological table with which three concepts are made. The characteristics of the chosen combination of solutions are:

1. **Minimize Cycle Time:** A combination of solutions that has the highest potential to shorten the process time.
2. **Compatible:** A combination of solutions that are best compatible with existing machinery.
3. **Affordable:** A combination of solutions that require the least amount of investment.

3.1.2. Decrease process time

In this subsection the solutions to decrease the process time are elaborated. First the solutions for a pressure system are shown and discussed. Second the solutions to increase the area where melting occurs are elaborated.

Pressure From the tests with the melting tube, as presented in subsection 2.1.1., it became evident that keeping pressure on the waste while melting decreases the process time. The pressure is beneficial as the WP waste seems to be well insulated against convection due to its high air/material ratio. By increasing the pressure on the WP waste in the Steimelt, more material is heated through conduction of the heating plates at the bottom of the Sterimelt. To increase the pressure $P = F/A$, two units are needed; force (F) and a surface (A). The morphological table in figure 3.2 shows different solutions to these units.

The solutions for force were divided into active and passive elements. The active elements need actuation during the melting process, whereas the passive elements do not need actuation during the melting process. The solutions indicated in red are solutions to the sub-problem, however they are not suitable for implementation in the Sterimelt and will not be considered for the conceptualisation.



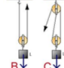
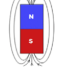









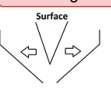
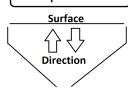
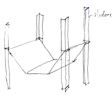
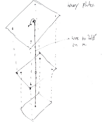

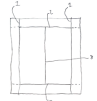
Pressure increase	
Force	
Active	Passive
<div style="display: flex; justify-content: space-around;"> <div>Mechanical </div> <div>Hydraulic/ Pneumatic </div> <div>Wire & pulleys </div> <div style="border: 1px solid red;">Magnetic </div> <div style="border: 1px solid red;">Combustion </div> <div style="border: 1px solid red;">Forced air </div> </div>	<div style="display: flex; justify-content: space-around;"> <div>Gravity/Weight </div> <div>Spring </div> </div>
<div style="display: flex; justify-content: space-between;"> <div>Extend range of motion / decrease space needed for actuators</div> <div>Correct end position</div> </div>	
<div style="display: flex; justify-content: space-around;"> <div>Lever </div> <div>Scissor </div> <div>Telescope </div> </div>	<div style="display: flex; justify-content: space-around;"> <div style="border: 1px solid red;">Sliding contacts </div> <div>Cables </div> </div>
Surface	
Direction of motion	
<div style="display: flex; justify-content: space-around;"> <div style="border: 1px solid red;">Left/Right </div> <div>Up/down </div> </div>	
Shape	
<div style="display: flex; justify-content: space-around;"> <div>Rigid end shape </div> <div style="border: 1px solid red;">Multiple, different sized square plates. </div> <div>Single, square plate </div> <div style="border: 1px solid red;">Foldable system </div> </div>	

Figure 3.2: Morphological table for pressure increase during melting. Red: Will not be considered for concepts.

Magnets are in red as magnets lose their magnetic field with an increase in temperature (Hopkinson et al., 1888). Moreover, the magnetic force decreases rapidly over distance due to the magnetic permeability of air (Lehner, 2010). Combustion poses a fire risk. A quick and simplified calculation shows that forced air is unrealistic as a means of force in the Sterimelt. The substitution of $P = F/A$ into the formula for dynamic pressure, in formula 3.1, and solving for the speed v gives formula 3.2. Where, F is the load of $400N$, A is the surface of a possible pressure plate of $0.6m^2$ and ρ is the density of air at $200^\circ C$ atm, which is $0.75kg/m^3$.

$$P = 1/2 * \rho * v^2 \quad (3.1)$$

$$v = \frac{2 * F}{A * \rho} \quad (3.2)$$

This yields a speed of $42m/s$. As most fans are rated by volumetric flow the speed is multiplied by the surface A , yielding $Q = 25m^3/s$. Implementing such a fan into the Sterimelt would leave no room for the WP waste. Due to the shape of the Sterimelts loading bay, see figure 1.1, some of the force solutions need extra constraints to ensure the correct end position is reached, for example gravity/weight. Whereas other solutions for force need an extended range of motion to reach the end position, for example hydraulic/pneumatic. In the category "Correct end position", in figure 3.2, sliding contacts are indicated in red as it is presumed that at the end of the melting cycle the plastic in the sliding contact solidifies. This would result in a rigid contact stopping the sliding contact from moving. This leaves the pressure system at the end position which makes reloading of the Sterimelt with WP waste sub-optimal. The direction of the surface in the left and right direction is in red as the heating plates of the Sterimelt do not extend to the full height of the loading bay. Therefore, part of the pressure on the waste would not result in an increase of melting. Finally, in the solutions for the shape, a foldable system is indicated in red. This solution would have to be made from compliant mechanisms as conventional hinges would also suffer from the solidification of the molten PP. Also, the complex shape of the loading bay of the Sterimelt makes it complex. Such a complex compliant mechanism is not in the scope of this project.

Melting zone Another means of decreasing melting cycle time is by increasing the area where melting occurs. The morphological table in figure 3.3 present the different solutions. Here forced convection is indicated in red, and will not be considered for the conceptualisation, as it is assumed the material has good resistance to convective heat. This is probably due to the high air to material ratio of WP waste and was noticed during the tests with the melting tube. Finally, radiation is red, as radiation becomes inefficient at higher temperatures (Ghajar and Yunus A. Cengel, 2014).

3.1.3. Pollution separation

To find solutions for separating the pollution from the PP in the WP waste. First a morphological table for the different phases was made. The solutions are separated by means of the physical principle through which the separation occurs. Figure 3.4 shows the morphological table for pollution separation, where the physical principles are in grey. Most of the red solutions are solutions that require large and expensive existing machinery. Furthermore, some of the red solutions cannot be used for all types of pollution found in the WP waste. For example, due to the small difference in density blow separation is not possible. Furthermore, now the pollution is separated by hand before the melting phase. This is represented by the block Human based, under manual. This leaves filtration as a solution. Another important aspect of filtration compared to human based is a more homogeneous end product. By

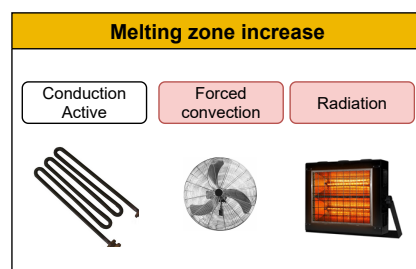


Figure 3.3: Morphological table melting zone. Red: Will not be considered for concepts.

Pollution separation	Before melting	During melting	After melting	
	Difference in density	Separate solid from liquid	Difference in density	
	Magnetic density separation		Magnetic density separation	
	Blow separation		Blow separation	
	Special liquid separation		Special liquid separation	
	Hydrophilic/Hydrophobic	Sedimentation	Evaporation	Distillation
	Flotation			
	Difference in charge	Centrifugation	Filtration	Chromatography
Electrostatic separation				
Manual				
Sensor based				
Human based				
Magnetic field				
Auxiliary		Sensor based		

Figure 3.4: Morphological table for pollution separation. Red: Will not be considered. Green: Will need further exploration.

placing a filter between the melting area and the end product tray, no unmolten material will be in the end product, see figure 1.2. To give a clear indication of the possibilities of filtration, a separate morphological table is made for filtration.

Filtration The tests with the melting tube, as presented in section 2.1.1., suggested that a double filter had the best flow properties. The first filter has only spikes to prevent large pieces of pollution from clogging the second filter. The second filter was perforated with 10 – 15mm holes, this ensured that even the smaller pieces of pollution were still filtered. With these observations a morphological table for a filtration system in the Sterimelt is made, see figure 3.5. Here the blocks with a yellow title are parameters that can be designed for. Efficiency is the cleaning capacity divided by the amount of space that can be used for waste. Heat distribution of the filter is needed to ensure the filter is hot, it is hypothesised that plastic flows better through a hotter filter. Two solutions were made for distributing the heat from the heating plates to the filter. The first, thick beams with good heat flow capabilities touch the sides. The filter will lay on top of these beams and will get heated through the heat flow of the beams through conduction. The second solution for heat distribution is making an extra tick filter and putting the ends on an angle. The sloped sides directly touches the heating plates distributing the heat. The shape and position of the filter are important aspects for the volume available for the waste. Here below the V, meaning below the heating plates, is in red as there is no room available between the heating plates and the tray of the end product. The material used for the filter needs to be considered for the mechanical load capacity, thermal conductivity, and weight of the filter. The shape through which the plastic flows has influence on the chances of pollution reaching the end product. Furthermore, the shape of the holes need to be taken into consideration for the flow through the filter. Larger holes likely increase the flow, however this can result in an increased chance of pollution in the end product.

3.1.4. Improved end product

Finally, the solutions for the complex end product are explored, see figure 3.6. The benefit of pelletizing is the homogeneous end product that is used in all injection moulding machines and the possibility of a continuous process. Unfortunately, pelletizing requires large machinery and a constant flow. It is worth mentioning that the other solutions for the complex end product need granulation after partitioning, to be implementable in an injection moulding machine. The granulator is present. As of now the end product in partitioned using a hydraulic press.

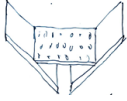

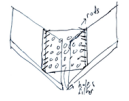
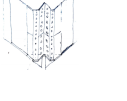
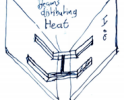
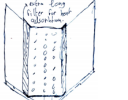

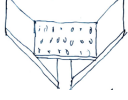
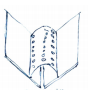
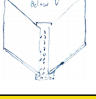

During melting: Filtration				
Efficiency				
One layer	Two layers	Two on one layer	Double channel	
				
Heat distribution				
Beams		Thicker and sloped		
				
Volume available for waste				
Convex	Flat	Concave		
				
Below V		In V		
				
Thermal conductivity and weight				
Gold	Copper	Steel	Alluminium	Stainless steel
Separation mechanism				
Lamellen	15 mm holes	Spikes	10 mm holes	Squares

Figure 3.5: Morphological table for filtration. Red: Will not be considered for concepts.

3.1.5. Conceptualisation

As the solutions are found for the different design goals, it is possible to form concepts. First, the different morphological tables per design goal are substituted into figure 3.1, at the beginning of this chapter. This substitution leads to one large morphological table, see figure 3.7. Subsequently, three concepts are made with the three characteristics presented at the top of figure 3.7. By following the arrows from these characteristics, different solutions are chosen to form concepts which are presented at the bottom of figure 3.7. In the following paragraphs the choices for the different concepts are





Improved end product	Partitioning of end product		Pelletizing during melting
	After melting	During melting	
	Saw 	Hydraulic 	Tray deviders 
			

Figure 3.6: Morphological table for the improved end product. Red: Will not be considered for concepts.

presented.

Minimize Cycle Time To limit the time of the melting cycle hydraulic/pneumatic in combination with scissors are chosen. Hydraulic actuators are chosen as a high force can be exerted with hydraulics. The scissors ensure that the pressure plate can reach the desired end position. It is assumed that scissors in combination with hydraulics is the least problematic with regards to solidifying of the molten waste. It is worth mentioning that hydraulics/pneumatic can be troublesome with large differences of temperature due to expansion of the hydraulic fluid/air. The scissors will actuate different sized plates to keep pressure on the WP waste over multiple levels of incline. The plates used for compression are actively heated with heating elements. Actively heating the plates will increase the area where melting occurs. For the separation of the pollution a single layer, but with two kinds of filtration will be used. The sides of the filter will have small spikes, which will stop the larger pieces of tape and sticker from reaching the permeable surface area. Beams are used for the heat distribution of the filter from the heating plates on the side. By using beams, the filter itself can be made thinner and lighter. The hypothesis is that a slimmer filter is easier and faster to replace. A downside of using beams for the heat distribution is that the filter will have a lower permeability. Flat is chosen as convex or concave in combination with beams would make the concept unnecessarily complex. The beams and filter are made of aluminium, because aluminium has better heat flow properties and is lighter than steel. Finally, the tray divider is used in the tray below to ensure the solidified blocks can directly be placed in the granulator.

Compatible For the pressure of the Compatible concept a set of plates with cables and weights are chosen. Using multiple plates makes it possible to keep pressure on the waste past multiple inclines of the Sterimelts loading bay. The cables are passive, ensuring a low complexity and are insensitive to solidifying waste. Another reason for choosing this combination is the limited amount of changes that are needed for implementation to the Sterimelt. The filtration is accomplished with a single sheet of aluminium that touches the heating plates on the side. The combination of an aluminium, thicker filter that touches the side is thought to have good heat flow properties. The increased thickness will also provide extra loading capacity. The sides of the plate will be fitted with spikes, like the cycle time design. Finally, the partition of the end product is done with a tray divider.

Affordable Finally, the Affordable concept will use a single plate on top of the WP waste to achieve pressure. The single plate will only compress the waste until a certain incline is reached. Filtration has been chosen for the affordable concept because manual removal of the pollution over a longer period is assumed to be more expensive than a basic filtration system. The filter will be made from stainless steel sheet material that is perforated with square holes. This kind of material is abundantly available at Van Straten Medical. Flat is chosen to reduce costs. Finally, the tray divider is chosen as it is assumed that manual partition of the end product with the hydraulic press will be more expensive over a longer period of time than a tray divider.

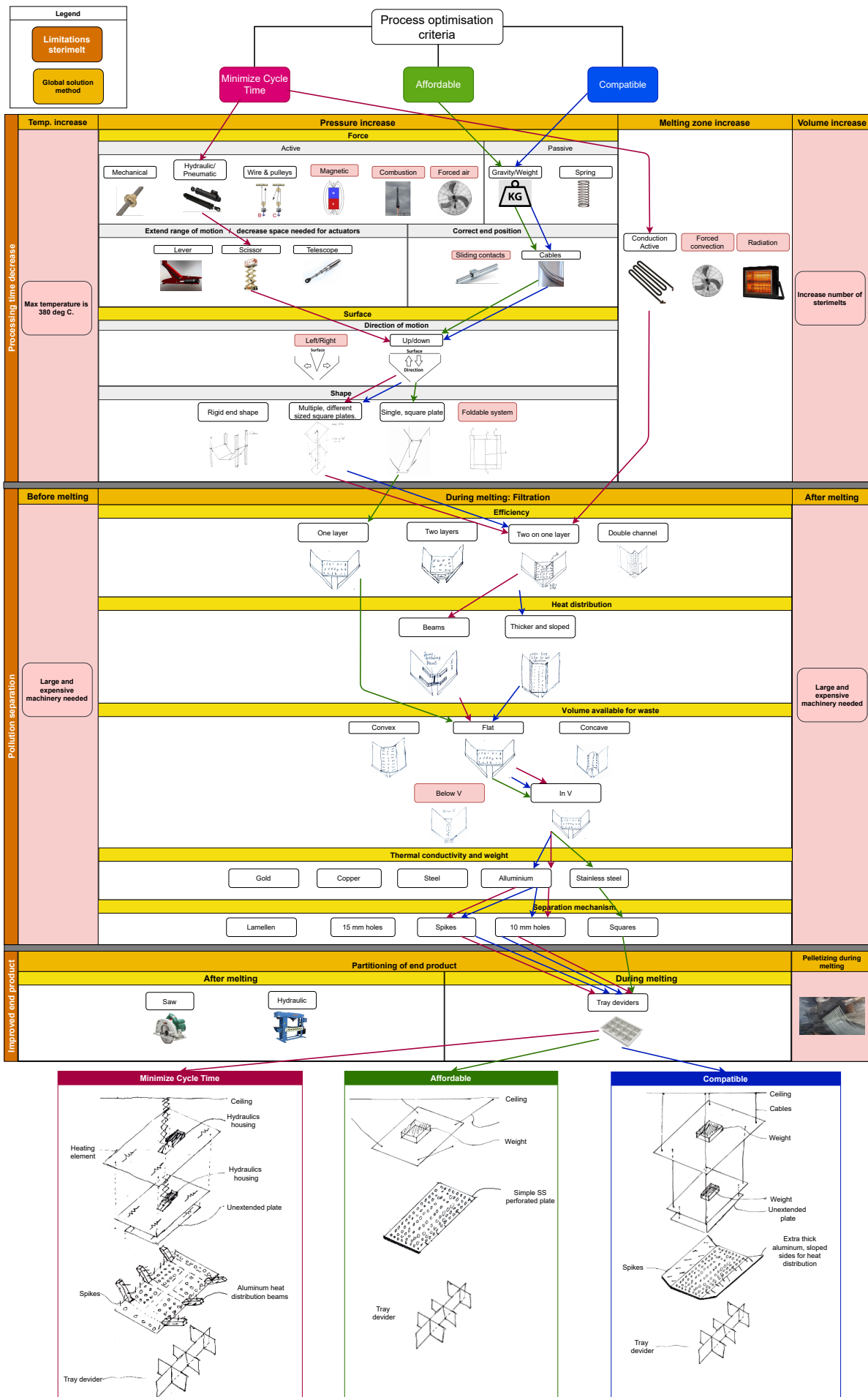


Figure 3.7: Morphological table for the process optimisation. At the bottom the resulting concepts are presented.

3.1.6. Conceptual evaluation

In this subsection the concepts are evaluated using thought experiments and a list of the key performance indicators (KPI). The list of KPIs and a short explanation can be found below. The KPIs were weighed from 1-3, where 3 is the most important. Next the different concepts, as presented in the bottom of figure 3.7, are graded from 1 to 10, with 10 being the highest.

1. **Add on to the Sterimelt:** No changes have to be made to the Sterimelt, e.g. electronics, drilling.
2. **Separate tape from PP:** Maximum of 1% pollution in the end product.
3. **Robust:** The solution has to be used at least 50 times.
4. **Flow:** Less plastic than pollution on the filter at the end of a cycle.
5. **Safety:** No exposure to surfaces hotter than 140°C and no toxic fumes.
6. **Mechanical load capacity:** The filter should not bend beyond its yielding point.
7. **Cost:** Modifications should cost less than 1000 euros.
8. **Operational needs:** When something breaks down the solution has to be out of order for less than a day.
9. **Temperature:** Temperatures should not differ more than 60°C, for more than 10 minutes at any point in the process.
10. **End product:** Should be directly implementable into the granulator.
11. **Weight:** The removable parts should weigh less than 5 kg.
12. **Cleanability:** Filter should be cleaned in 30 min.

In table 3.1 the grade per KPI for each concept can be found in a PUGH matrix. Only using the KPIs available with thought experiments the Affordable concept would score the highest with a 8.9. However, with half of the KPIs not included, as they need tests, no conclusion can be drawn from this evaluation. To be able to make a good comparison between the different concepts, some KPIs will be assessed with tests. Unfortunately, there is only a limited amount of time available for a thesis project. Therefore, it was chosen to;

- Prototype the filtration system of each concept.
- Assess pressure on a conceptual level.
- Make and asses the tray divider.

A prototype in this context means that only 1/3 of the filter will be created to assess the filter. Prototyping the filtration systems makes it possible to evaluate the KPIs; Separate pollution, Flow, Mechanical load capacity, Temperature and Cleanability with tests. As all concepts rely on a pressure system to decrease the cycle time it was chosen to asses pressure on a conceptual level. Finally, the tray divider is developed to see if this addition can decrease the process time.

Table 3.1: PUGH matrix for the conceptual evaluation of the concepts; Minimize Cycle Time, Compatible and Affordable. Final column: Indicates which Key Performance Indicator (KPI) will be tested for a proper evaluation. Bottom row: Grade of the concepts without the to be tested KPIs.

Key performance indicator	Weight	Minimize Cycle Time	Compatible	Affordable	Notes
Add on to Sterimelt	3	4	7	10	
Separate pollution	3	0	0	0	Will be tested
Robust	3	2	8	8	
Flow	3	0	0	0	Will be tested
Safety	3	4	6	8	
Mechanical load capacity	3	0	0	0	Will be tested
Cost	2	1	8	10	
Operational needs	2	3	8	10	
Temperature	2	0	0	0	Will be tested
End product	2	0	0	0	Will be tested
Weight	1	8	4	7	
Cleanability	1	0	0	0	Will be tested
Grade:		3.3	7.1	8.9	

3.1.7. Tests for evaluation

In this subsection the test protocols to evaluate the KPIs that need tests for proper evaluation are elaborated. To test the filtration systems and pressure the loading bay, where the WP waste is loaded, and the tray with the resulting end product are split up in three compartments, see figure 3.8. This is done to ensure, that a good comparison can be made between the different filters.



Figure 3.8: Test setup in the Sterimelt. Top left to bottom; Top view of loading bay with dividers, Loaded loading bay with clean WP waste and loading bay dividers, Side view of loading bay with dividers, End product tray with the tray divider used for testing.

Separate pollution To analyse if the filters separate the pollution sufficiently. Each compartment of the loading bay is filled with 2 kg of polluted WP waste. A melting cycle of: 25 min warming up to 300°C, 40 min steady state, 35 min cooldown cycle. After the melting cycle, the resulting blocks are visually inspected for pollution. The assumption is that in a batch of 2 kg WP waste the same amount of pollution is present. The test will be done three times, each time the filters will be placed in a different location. This is to ensure the location has no influence on the results.

Flow As flow is critical for the cycle time two tests are done.

Polluted WP waste In the first test the loading bay compartments are filled with 2 kg of polluted WP waste. A melting cycle of: 25 min warming up to 300°C, 40 min steady state, 35 min cooldown cycle. Afterwards the filter will be examined on its permeability. The permeability will be calculated as the permeable surface after melting divided by the total surface of the filter, which is equal for each filter as they all span 1/3 of the Sterimelt. This test will also be done three times, for the same reasons as above.

Clean WP waste For the second test each loading bay compartment is filled with 2 kg of clean WP waste. A melting cycle of: 25 min warming up to 300°C, 11 min steady state, 35 min cooldown. The shorter steady state will leave some of the plastic unmolten. Afterwards, the filters and the remaining plastic are weighed and compared to the weight of the filter before testing. This test will also be done three times, for the same reasons as above.

Mechanical load capacity To analyse if the filters do not plastically deform during the melting cycle, a FEM analysis is conducted in Solidworks. The FEM analysis in Solidworks is done to make sure the yielding stress is not reached with four times the load. Four times the load is chosen to ensure the filtration system would be able to handle the extra pressure of a possible pressure system. An elaborate calculation of the load can be found below. A correction is done for the Minimise Cycle Time and Compatible prototypes as they are made of aluminium. The material properties of aluminium decrease due to the increased temperature, this is further elaborated below. Because of these changes in material properties, it was chosen to require the aluminium prototypes to have a safety factor between 5-10 times the yield stress. The stainless-steel prototype should suffice with a safety factor of 3-5 times the yield stress, as the material is less affected by heat.

The total load on the filter is 21kg, this is the weight of the end product from a fully loaded cycle. The load is multiplied by four to include a possible pressure system. As the prototypes span only one third of the loading bay, the load is multiplied by 1/3. The widths of the prototypes is 200mm, this is chosen based on capacity of the loading bay. The filters are not made slimmer as it hypothesised that the chance of a full blockage of the filter, due to the pollution in the waste, will become too high. Part of the load is on the inclined heating plates. This will be considered with a loading ratio for the geometry, see formula 3.3. The length between the side plates at the top is 800mm, this leaves 300mm on each side for the inclined heating plates, indicated by $width_{incline}$ in formula 3.3. Assuming the load to be uniform uniform yields the following equation:

$$Ratio_{geometry} = \frac{width_{filter} * h}{2 * 1/2 * width_{incline} + width_{filter} * h} = 0.4[-] \quad (3.3)$$

The load is modelled downwards on the top face of the filter in Solidworks. The total load calculation can be found in equation 3.4.

$$Load_{waste} = 4 * length_{prototype} * weight_{endproduct} * g = 4 * \frac{1}{3} * 0.4 * 21 * 9.81 = 110[N] \quad (3.4)$$

The material used for the filtration systems of the Compatible and Minimizing Cycle Time is aluminium. The Sterimelt is set to reach a temperature of 300°C during the melting cycle. This is approximately half of the melting temperature of aluminium. The elevated temperature leads to changes in the material properties and must be accounted for during analyses. The filters will be made from commercially available 1050H14/H24 aluminium. The beams for the Minimizing Cycle Time concept will be made from 6030T5 aluminium. A study by Su and Young, 2019 shows the changes to the material

Table 3.2: Reduction factors of the material properties, used for the FEM analyses of the aluminium prototypes at elevated temperatures.

Reduction factors aluminium T6063	
Temperature [C]	300
Youngs	0.75
Yield stress	0.68
Ultimate stress	0.60

properties of 6030T5 at elevated temperatures, see table 3.2. Unfortunately, no study was found on the material properties of 1050H14/H24 aluminium at elevated temperatures. Therefore it is decided to use the same reduction factors for the 1050H14/H24 aluminium as found for the 6030T5 aluminium. The Affordable concept uses stainless steel, which has melting temperature of about 1400°C . It is generally accepted that the material properties of stainless steel are unaffected up until 500°C . Therefore, the Affordable concept suffers no material changes during the melting cycle and has lower requirement of the safety factor.

Finally, the constraints as implemented in Solidworks are shown in figure 3.9. The prototypes all have a face roller/slider contact indicated in red. This constraint ensures the part does not move along its length during the simulation, while at the same time producing the correct bending moments. The faces and lines highlighted in blue are only constraint in the plane of the heating plates, this is done on both sides. For the Affordable concept two planes are made to simulate the constraint of the heating plates of the Sterimelt, as no surfaces are present in that plane.

Temperature To analyse if the filters differ more than 60°C for more than 10 minutes with the heating plates, an infrared camera is used. The camera will be placed in the plane of the door of the Sterimelt, 2m above the floor of the Sterimelt. Black electrical tape is used to minimize the effects of reflection. The tape spans across the width of the filter and is placed with 50mm increments. A melting cycle of: 12 min warmup up to 200°C , 11 min steady state, 12 min cooldown is used. During this cycle a photo will be made every 3 minutes. This test is done separately for each filter to ensure the location of the filter has no influence.

For the measurement of the temperature, each filter was placed separately in the middle of the Sterimelt. Using the software FLIR-tools, lines were placed over the photos. Line 1 is used to calculate the temperature of the heating plate on the right, line 2 is used to calculate the temperature of the left heating plate, lines 3,4,5 and 6 are used to calculate the temperature in the middle of the filter. As

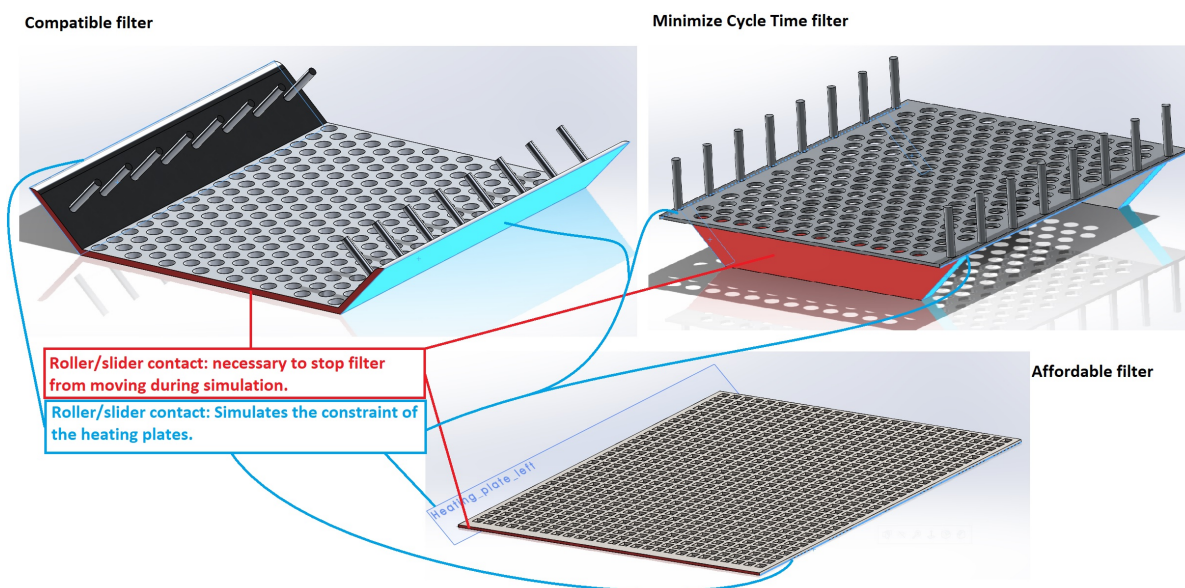


Figure 3.9: Constraint on the models of the filters used in Solidworks.

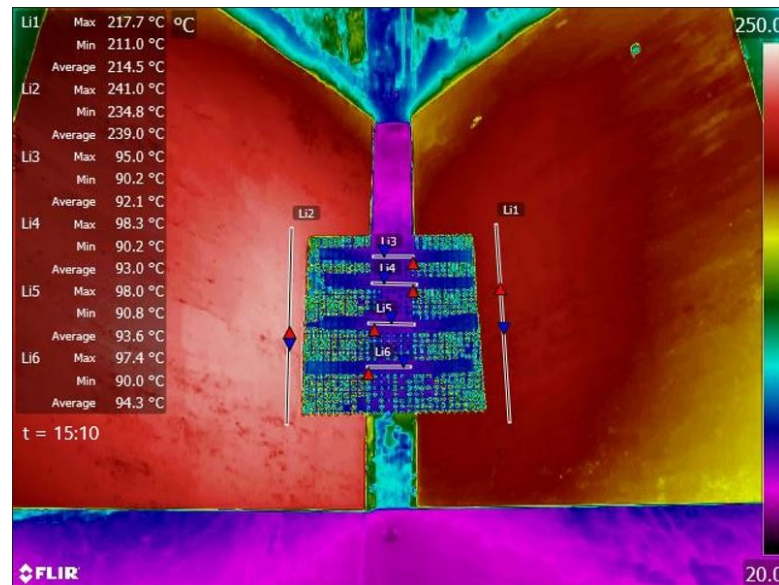


Figure 3.10: Example of line placement in FLIR-tools on the Affordable filter. The pixels which contain the temperature on the lines, are extracted and used for data processing. Temperature scale on the right in °C.

heating comes from the heated side plates, it is assumed that the middle is the coldest point of the filter. Lines 3,4,5 and 6 are placed on the black electrical tape to ensure minimal effects of reflectivity. Furthermore, the middle lines are placed over the slit in the Sterimelt where no heating plates are present. This is done to reduce to effects of the convection on the electrical tape from the heating plates below. The Matlab code used for processing the data can be found in appendix C.

End product To assess if the tray divider partition the end product sufficiently, such that the end product is directly implantable in a granulator. The tray divider is made and used on a full load of about 21 kg of WP waste. Having a cycle time of: 40 min warmup up to 350°C, 50 min steady state, and 40 min cooldown. After the end product is fully solidified it is separated from the tray dividers and placed in a granulator.

Cleanability The cleanability will be measured as the time needed to remove all pollution from the filter. The cleaning is done with a heat gun and scrapers. The heat gun is needed to break the bond of the adhesive tape on the filter. The heat gun's temperature will be set at a maximum of 300 °C to ensure that no other deformation than during melting occurs.

Pressure To analyse if pressure is a viable option to decrease the melting time, one compartment is filled with 2 kg of clean WP waste. A melting cycle of: 20 min warm up up to 250°C, 11 min steady state, 25 min cooldown. The shorter steady state will leave part of the plastic unmolten. Afterwards, the filter with unmolten plastic is weighed and compared to the weight of the filter before the cycle. The same test is repeated, but now with an aluminium sheet of 8mm thick, 240mm long and 400mm wide on top. A significant difference in weight of unmolten plastic between the first and second test will determine if pressure is a viable option. The test setup for the pressure test can be found in figure 3.11.



Figure 3.11: Test setup used to analyse if pressure is a viable option for decreasing the cycle time of the Sterimelt.

3.2. Results

With the test protocols for KPIs defined the prototypes can be properly evaluated. In this section the resulting prototypes are first dimensioned. Subsequently, the result of the tests are presented. Finally, the concepts are reevaluated with the insights gained from the tests.

3.2.1. Prototypes

First, the dimensions and the resulting filter prototypes are presented. Subsequently, the tray divider is dimensioned and presented.

Filter: Minimize Cycle Time The filter for the Minimize Cycle Time prototype uses beams that are made of $30\text{mm} \times 10\text{mm}$ 6030T5 aluminium profile. The beams form an I profile, when seen from above, with a length and width of 200mm . The aim of the beams is to distribute the heat from the heating plates while also supporting the filter. This extra support should make it possible to make the actual filter thinner without it breaking. The hypothesis is that a lighter filter is easier and quicker to replace. The filter is made from a 2mm thick sheet of 1050H14/H24 aluminium alloy, perforated with 10mm diameter holes separated at 15mm at a 60° angle. The filter is 240mm long and 200mm wide, this is just short of 250mm ($1/3$ of the length of the loading bay). The shorter length is to leave some space for the bay loading bay dividers. The side of the filter is equipped with 5mm diameter aluminium rods with a length of 30mm that are spaced 30mm apart, see figure 3.12.

Filter: Compatible The filtration prototype for the Compatible concept is made of a single 4mm thick sheet of aluminium 1050H14/H24 alloy. The sheet is 300mm wide, the sides of the sheet are bend at an 45° angle. The horizontal 200mm part of the sheet is perforated with 10mm diameter holes separated at 15mm and at a 60° angle. The bent sides are equipped with 5mm diameter, 30mm long rods spaced 30mm apart, see figure 3.12.

Filter: Affordable The affordable prototype is made of 1.5mm thick, 200mm wide and 240mm long, sheet of stainless steel. It has square holes of $5 \times 5\text{mm}$ spaced 7.5mm apart, see figure 3.12.

Tray divider The tray divider is made from one 1.2mm thick, 885mm long and 120mm wide sheet of stainless steel. The top and bottom side of the sheet has 60mm long slits of 1.5mm wide spaced 75mm apart. These slits are used to place 265mm wide and 120mm long stainless-steel sheets of 1.2mm thick. These smaller stainless-steel sheets have the same kind of slits, interlocking the both in place. Point welds are at the bottom and top, to prevent the sheets rotating along the axis of the slits, see figure 3.12.

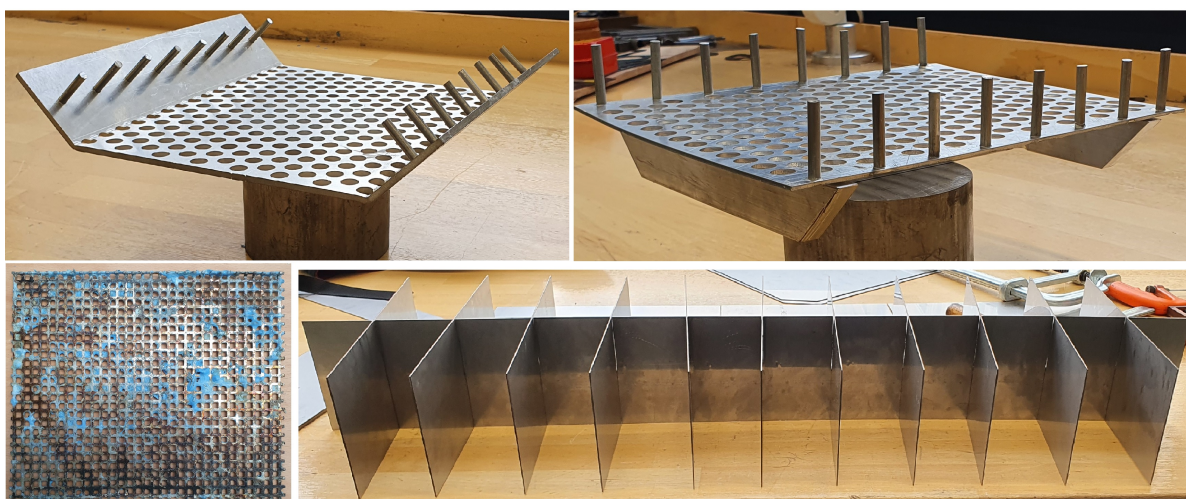


Figure 3.12: Prototypes. From top left to bottom right; Compatible filter, Minimize Cycle Time filter, Affordable filter and tray divider.

3.2.2. Test results

In this subsection the results of the tests for the evaluation of the certain KPIs are presented.

Separate pollution After the three tests for pollution only the Minimize Cycle Time, after one test, had pollution in the end product, see figure 3.13. The other eight end products, three for each filter, had no visual pollution in the end product. Per test the filters were placed at different locations. Such that all filters were tested on all locations, this ensured that the location of the filter had no influence on the results. The other brown spots on the block are not stickers and tape, these are probably the result of melted glue residue from the stickers and tape.

Flow: Polluted WP waste The first test to measure flow is measuring the permeability after the melting of polluted WP waste. The permeable surface in %, as presented in table 3.3, is defined as the surface free from flow divided by the total horizontal surface of the filter, which is equal for each filter. Moreover, the results are the average over three tests. Per test the filters were placed at different locations such that all filters were tested on all location. This ensured that the location of the filter had no influence on the results. The results show that the Compatible filter has the highest average permeable surface after tests with polluted material, despite the fact it has the lowest amount of permeable surface before the test.

Flow: Clean WP waste For the second test on flow the filters were weighed before and after a short melting cycle with clean WP waste. The test was repeated thrice, for the same reasons as the previous tests. The average over the tests is presented in table 3.4. The Compatible filter has the lowest amount of unmolten plastic weight after the melting cycle.

Mechanical load capacity For the Mechanical load capacity of the filters the FEM analyses with the constraint, load and material properties, as presented in subsection 3.1.7, were simulated. The safety factors can be found in table 3.5 and the stress profile on the deformed filters can be found in Appendix D. All filters suffice according to the required safety factor.

Table 3.3: Average Permeable surface before and after three tests with polluted WP waste. Presented as a percentage of the total horizontal surface of the filter, which is equal for each filter.

Filter	Permeable surface pre-test [%]	Permeable surface post-test [%]
Minimize Cycle Time	39%	9%
Compatible	38%	12%
Affordable	42%	3%

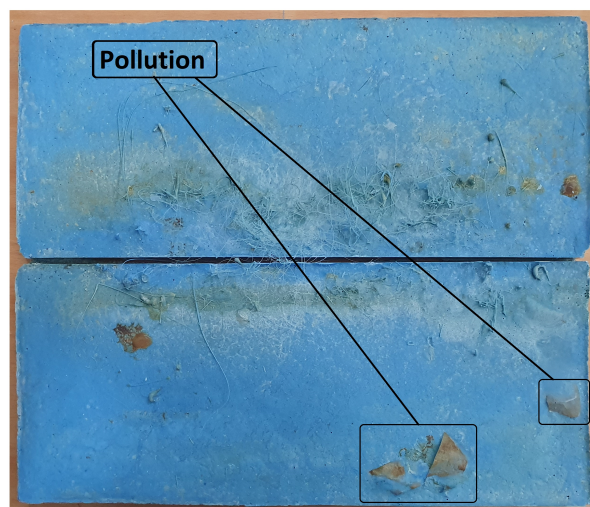


Figure 3.13: Pollution found once in the end product of the Minimize Cycle Time prototype. The other brown spots is likely glue residue from the tape and stickers.

Table 3.4: Average weight before and after three short cycle tests with clean WP waste.

Filter	Weight before [gr]	Weight after [gr]	Weight unmolten WP [gr]
Minimize Cycle Time	618	945	327
Compatible	620	697	77
Affordable	323	627	303

Table 3.5: Stress and deformation profile from the FEM analyses in Solidworks.

Filter	vonMises max stress [Mpa]	Yield strength [Mpa]	Safety Factor [-]
Minimize Cycle Time	6.85	61.2	8.9
Compatible	8.19	61.2	7.5
Affordable	62.6	172	2.7

Temperature The results from the IR temperature tests are plotted in the figure 3.14. It is worth mentioning that the figure in the bottom right has a different temperature scale. The line ambient temperature was read from the display on the Sterimelt. A boxplot is made for each time step to show the variation in temperature per measurement. The bottom right graph in figure 3.14 shows the Compatible filter becomes the hottest.

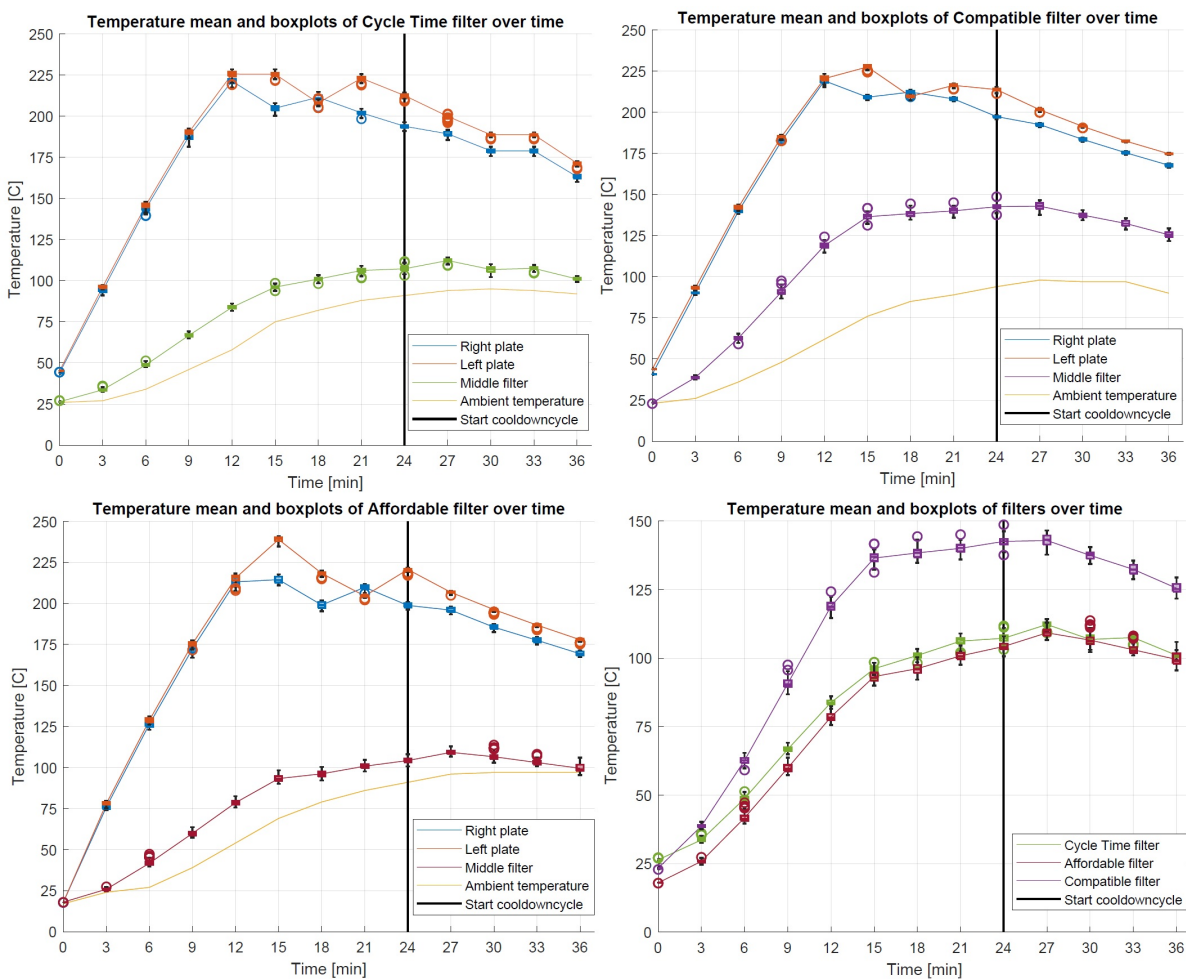


Figure 3.14: Temperature, measured with an IR-camera, plotted over time. Top left to bottom right: Temperature profile of the Minimize Cycle Time filter, Temperature profile of the Compatible filter, Temperature profile of the Affordable filter, Temperature profile of the filters combined in one graph.



Figure 3.15: Tray with tray divider after a melting cycle.

End product The partitioning of the end product was successful in the sense that the resulting blocks, when fully hardened, could be placed directly into the granulator. This means that the manual partition of the larger blocks, with a hydraulic press, is no longer necessary. The resulting end product with tray divider can be found in figure 3.15.

Cleanability In figure 3.16 the Affordable filter can be seen before and after cleaning. Not all plastic was removed, however all pollution was removed. It is assumed that as long as all pollution is removed the filter has the same flow characteristics as before testing. The results per filter per test are summarised the table 3.6. The Compatible filter takes the longest time to clean while the Affordable filter is cleaned the fastest.

Pressure For the pressure test the Compatible filter was weighed before and after the melting cycle of clean WP waste. The Compatible filter was used as it became clear, from previous tests, that the compatible filter had the most favourable flow characteristics. The results are summarised in table 3.7 the extra pressure yielded a weight reduction in unmolten plastic of 40%.

Table 3.6: Time needed to remove all pollution from filter.

Filter	Test 1	Test 2	Test 3	Average
	Time [mm:ss]	Time [mm:ss]	Time [mm:ss]	Time [mm:ss]
Minimize Cycle Time	13:23	08:50	14:33	12:15
Compatible	23:47	20:12	15:01	19:40
Affordable	10:02	11:46	12:31	11:26

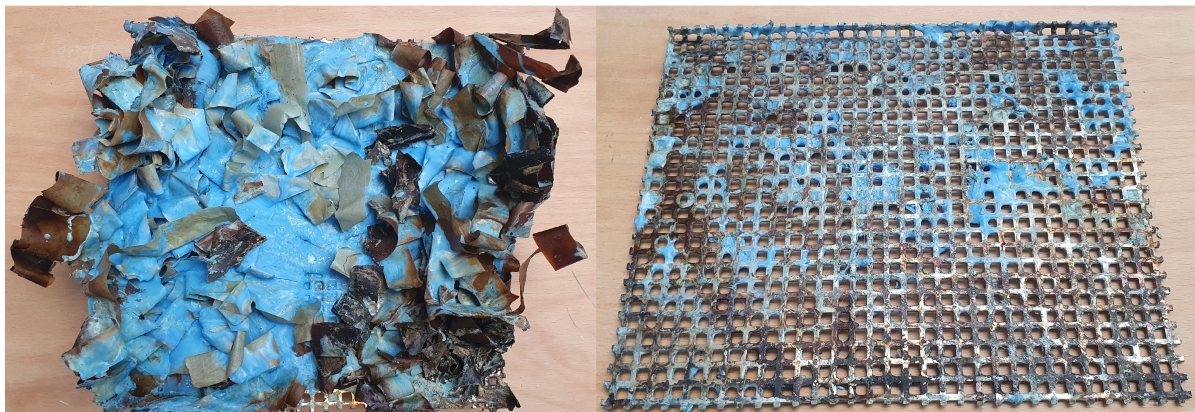


Figure 3.16: Left: Affordable filter before cleaning. Right: Affordable filter after cleaning.

Table 3.7: Summerized results of the conceptual test with and without pressure.

Scenario	Weight before [gr]	Weight after [gr]	Difference in weight [gr]
Compatible without pressure	615	1140	525
Compatible with pressure	610	925	315
		Difference in %	-40%

3.2.3. Reevaluation

In this subsection the concepts are reevaluated and the grades of the tested KPIs are shortly explained. The grades on the tested KPIs are a combination of the results, as presented in subsection 3.2.2, and practical insights gained while using with the filters. The results are summarised in table 3.8.

Separate pollution The grades for the KPI Separate pollution of the Minimize Cycle Time and Compatible concepts are in line with the results from the previous section. However, the Affordable concept scores relatively low even though no pollution was found in the end product. The lower grade is assigned because the filter regularly moved while loading the Sterimelt with WP waste.

Flow The grade for the KPI Flow is a combination of both flow test results. The Compatible filter concept had the highest amount of permeable surface and the lowest amount of unmolten weight. The Minimize Cycle Time had the same amount of unmolten weight as the Affordable concept. However, the Minimize Cycle Time concept surpassed the Affordable concept in permeable surface.

Mechanical load capacity All prototypes sufficed the safety factor criteria for the mechanical load capacity. However, during cleaning of the Minimize Cycle Time concept it was noticed that the top layer of the filter bent regularly, thus scoring lower.

Temperature The grades for the KPI Temperature are solely based on the results from the IR temperature measurements.

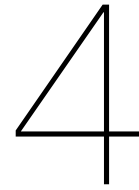
End product All concepts had the same solution of the end product and thus scored the same. However, the highest score was not given as the end product with tray divider took longer to solidify.

Cleanability The concept Minimize Cycle Time scores lower than the Affordable concept even though the time to clean the filters was roughly the same. This lower grade is because the Minimize Cycle Time filter had to be handled with extra care to prevent it from bending.

Table 3.8: PUGH matrix for the reevaluation of the concepts; Minimize Cycle Time, Compatible and Affordable. Final column: Indicates which Key Performance Indicator (KPI) have been tested for reevaluation. Bottom row: Grade of the concepts after reevaluation.

Key performance indicator	Weight	Minimize Cycle Time	Compatible	Affordable	Notes
Add on to Sterimelt	3	4	7	10	
Separate pollution	3	4	10	6	Tested
Robust	3	2	8	8	
Flow	3	6	10	1	Tested
Safety	3	4	6	8	
Mechanical load capacity	3	6	9	9	Tested
Cost	2	1	8	10	
Operational needs	2	3	8	10	
Temperature	2	4	10	4	Tested
End product	2	8	8	8	Tested
Weight	1	8	4	7	
Cleanability	1	6	1	8	Tested
Grade:		4.4	8.0	7.3	

To conclude the reevaluation of the concepts the KPIs are summarised in a final grade at the bottom of table 3.8. The Compatible concept has the highest grade of 8.0 closely followed by the Affordable concept with 7.3. Finally the Minimize Cycle time scores relatively low with a 4.4.



Discussion

In this section the results are discussed. First the results on the material properties are discussed. Second the results for optimizing the melting process are examined. Finally recommendations for future work and limitations of the study are made.

4.1. Material properties of the recyclate

The goal of the first part of this study was to investigate if high quality PP, for the use of injection moulding, can be made from blue wrapping paper waste. To test the material properties, various dog-bones were made and tested with tensile tests.

The temperature at which the WP waste was melted, before granulation, did not significantly influence the material properties of the injection moulded product. Other studies on the recyclability of PP report rapid material degradation with higher initial melting temperatures as well as reporting that the addition of virgin material can significantly reduce this effect (da Costa et al., 2007). However, this study found that the melting temperature of 250°C gave only marginal beneficial results.

The influence of the mixing ratios of virgin material with the recycled granulate was investigated, the results are summarized in figure 2.4. The results suggest that the mixing ratio has a strong influence on the material properties. As reported in previous studies, the injection moulded product made from recycled PP behaved in a more brittle manner making it harder and stiffer when compared to products made from virgin PP (da Costa et al., 2007; Hyie et al., 2020). This does not imply a lesser product, rather a different product. Different applications require different material properties, as such the mixing ratio can be adapted according to the applications needs. When comparing 50%R and virgin material the results show that the UTS increased by 6%, the strain at break decreased by 17% and the Youngs modulus increased by 11%. These results imply that material degradation of the samples made with a mixing ratio of 50%R were limited when compared to virgin samples. As stresses found in the bulk of plastic products are within their elastic deformation domain, 50%R is a viable option for most PP products. Furthermore, it can be concluded that the mixing ratio has a stronger influence on the strain at break than on the UTS and Youngs modulus.

Finally, the results of the 100%R and the polluted samples are compared with virgin material. The UTS decreased by 5% and the strain at break decreased by 59% of the polluted samples when compared to the virgin. Whereas the UTS increased by 16% and the strain at break decreased by 42% when comparing 100%R with virgin material. These results show that recycling with pollution not only has a negative effect on the strain at break, as with clean 100%R, but also on the UTS. Pollution has a limited effect on the Youngs Modulus. The degradation of the UTS can be explained by the pollution. The pollution decreases the amount of effective surface area where stress is applied on the plastic dog bone.

4.2. Remelting process optimisation

The goal of the second part of this study was to investigate how the remelting process could be optimized to minimize the time to make 99% pure PP granulate from WP waste. Three concepts were made and scores were assigned to different KPIs. Certain KPIs were evaluated with prototypes of the

filters. Pressure as a means of decreasing the melting time was evaluated on a conceptual level. The results of these tests are discussed below.

Only the prototype Minimize Cycle Time had visible pollution in the end product. This only occurred during one of the tests with polluted WP, suggests the pollution was due to misplacement of the filter. The misplacement is inherent to the design of the Minimize Cycle Time because the light top layer, which rests on the beams, is prone to move during loading.

From the results on the permeable surface in table 3.3 it can be concluded that the Compatible filter suffers the least from pollution. From the difference in permeable surface between the Minimize Cycle Time and Compatible filter, it can be concluded that putting the spikes on an incline away from the permeable surface makes it less likely for the stickers and tape to clog the filter.

The results for melting clean wrapping paper showed that the Compatible filter yielded the least amount of unmolten plastic. This was the first indication that the Compatible filter had the best heat flow characteristics.

The designed prototypes all met the condition with regards to their mechanical loading capacity. The top of the prototype Minimize Cycle Time could have been made from 1.5mm aluminium and still meet the criteria. It was chosen to make the filter 2mm to ensure better heat flow and extra mechanical loading capacity. In hindsight it was the right decision, as during the cleaning the filter was bent quite easily.

The temperature tests, summarised in figure 3.14, suggest that the Compatible filter has the best heat flow characteristics as it became the warmest. The results of the temperature analyses also suggest that the Compatible filter follows the temperature of the heating plates, whereas the Minimize Cycle Time and Affordable filter temperatures are closer to that of the ambient temperatures. The flattening of the temperature curve of the Compatible filter is common for systems that reach a steady state. Here the steady state is reached as the amount of heat input, from the heating plates, is equal to the amount of heat lost to the ambient atmosphere. The larger variation in temperature of the Compatible filter is due to the larger holes and larger temperature difference with the ambient temperature, when compared to the other filters. The relatively low temperature of the Minimize Cycle Time filter could be attributed to the fact that the top of the filter did not touch the beams everywhere. To distribute the heat via the beams, it is important that the filter and beams touch everywhere. Unfortunately, this was practically impossible.

The partitioning of the end product was successful as the end product was directly implementable into the granulator. Without the tray divider it was possible to empty the tray when the outside of the end product was hardened. However, the tray divider is in the middle of the end product, therefore one has to wait till the whole end product is hardened before emptying the tray.

The Compatible filter took the longest to clean, almost twice as long as the other two filters. The longer cleaning time may be explained by its complex shape, making it harder to hold while cleaning. Furthermore, due to the thickness of the filter (4mm) it took longer to warm up the filter and melt the boundary layer between the residue on the filter and the filter itself. While the cleaning of the filter took longer than expected, it is still less time consuming to clean the filters than to clean the sheets manually. Furthermore, it is speculated that it is easier to design a machine to clean the filter than it is to design a machine to remove the stickers and tape from the WP waste.

Finally, pressure yielded a weight reduction of 40% compared to a test without pressure. For pressure to decrease the melting cycle time it is important that the filter has adequate heat flow and plastic flow properties. Otherwise, the extra pressure will be on a cold filter which will not result in more plastic being molten.

4.3. Recommendations & limitations

In this section first recommendations on the results for the material properties are done. Secondly, recommendations on decreasing the process time are given. Finally, the recommendations on the project as a whole are presented.

One of the batches melted at 250°C was in the oven for almost double the time needed to melt the plastic. This resulted in very poor material properties. Furthermore, when mixing this “bad” batch with virgin plastic the material properties were like that of the batch with a normal melting time. It is therefore recommended to further analyse the influence of the time that the WP waste is at elevated temperature and how this time effects the material properties. Furthermore, the influence of virgin material to

reverse said effects should be analysed. It is recommended to do these tests with the end product of the Sterimelt, as this is the oven used on industrial scale.

The SD of the strain at break of the washed 100%R samples (SD2.4) and the samples made from 100%R without washing (SD 0.7) differed significantly. However, with a sample size of at three for the washed samples it is not possible to assign this larger SD to the washing cycle. It is therefore recommended to do the same test with more samples to see if the larger SD is due to the washing and not a sampling error.

The standard settings for remelting WP waste with the Sterimelt is at a temperature of 360°C. This study only looked at the material properties of WP remelted up to 300°C. For future studies it is recommended to analyse at the material properties, with the mixing of virgin material, of WP waste remelted at 360°C using the Sterimelt. By doing this the influence of the Sterimelts remelting temperature on the material properties can be analysed.

A simple solution to the longer time needed before a tray with divider in it can be emptied is buying two more trays. By doing this the end products can harden overnight.

In case a full-scale Compatible filter is built, it is recommended to extend the inclined plates for the use of extra and longer spikes. The extra spikes are necessary as a fully loaded Sterimelt has larger amounts of WP and pollution. Furthermore, to decrease the time needed to clean the Compatible filter it is recommended to first uniformly heat the filter after which the residue should be easily removable with a brush. A special coating could make the residue easier to remove.

Finally, study demonstrated that the recycling of PP is possible and has a limited effect on the material properties. It would be interesting to see what other large plastic streams (PET, PVC) from the OR could be recycled (McGain et al., 2009;McGain et al., 2015).

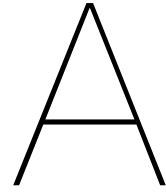
5

Conclusion

The objective of this study is to acquire high quality PP, for the use of injection moulding, from blue wrapping paper waste as well as analysing and proposing solutions for optimizing the melting process.

The results of this study show the effects on the material properties of recycling WP waste. The melting temperature did not significantly change the material properties. The recycled PP behaves in a more brittle manner, with the strain at break decreasing and the Youngs modulus and UTS increasing. Furthermore, these changes in material properties can be reduced by mixing virgin material with the recycle. Pollution in the material showed a reduction in strain at break, UTS and Youngs modulus. The influence of the CSSD washing cycle on the material properties was analysed for the use of a new instrument opener. The results show minimal material changes even after ten washing cycles. From the results of this study, it can be concluded that high quality PP can be acquired from WP waste.

To decrease the time needed to obtain 99% pure PP granulate from WP waste the melting process was analysed. The reduction of the cycle time by means of pressure was analysed on a conceptual level and showed promising results. The separation of the pollution from the WP during the melting cycle with filtration was tested with three different filter designs. The results show that good heat flow through the filters is important for reducing the melting cycle time. Filtration significantly reduces the time needed to obtain 99% pure PP compared to manual removal of the pollution. Partitioning of the end product with a tray divider made the end product directly implementable in a granulator. From these results it can be concluded that adding a pressure system, a filtration system and a tray divider can reduce the process time for obtaining 99% pure granulate from WP waste.



Matlab code: material properties

Contents

- Import data
- Example of processing data for Virgin N=7

Import data

```
clear; close all;
% make vectors used for reading the data
names1 = 1:1:25;
names2 = 148:1:172;
N_rows = 350;
%assign space for imported data
imported_data = nan(N_rows,8,25);

% fill a vector with names and import the files. Importfile is a matlab
% created function.
for i = 1 : length(names1)

    filename{i,1} = strcat('trekdogbone30032021',num2str(names1(i))...
    ,'_',num2str(names2(i)),'.TRA');
    data_sample = table2array(importfile(filename{i,1},2,N_rows));
    imported_data(1:length(data_sample),:,i) = data_sample;
end

% Adding stress and strain
% surface and zero length
A = 0.006*0.002*1e6;           %mm^2
L0= (0.040-2*0.0052)*1e3;     %mm

% collumn 6 becomes strain dL/L 9h in %
imported_data(:,6,:) = imported_data(:,5,:)/L0;
% make collumn 9 stress MPa
imported_data(:,9,:) = imported_data(:,4,:)/A;
```

Example of processing data for Virgin N=7

```
%select data, N = 7, #15 excluded: bad data
data_virg(:, :,1) = imported_data(:, :,33);
data_virg(:, :,2:7) = imported_data(:, :,35:40);
% assign place, use nan for mean and std.
virg      = nan(300,10,7);
```

```

finals      = zeros(7,1);
%Used for plot
error      = nan(20,7);

for j = 1 : 7      %imported_data(k,1,1) > 0
    % Find start and end of interesting data
    % start is first value greater than 0
    start = find(data_virg(:,9,j) >= 0,1, 'first');
    [Max,I] = max(data_virg(start:end,9,j));

    % save max stress is also end of data.
    virg(1,10,j) = Max;
    final      = I + start;
    finals(j,1) = I;

    % save max strain
    virg(2,10,j) = data_virg(final,6,j);

    % Put in a separate matrix with NaN for mean and std.
    virg(1:final-start+1,1:9,j) = data_virg(start:final,1:9,j);

    % change these if want to start and finish at different points
    % start search at 0.05 percent strain and stop at 1%
    begin_E_search = 0.05/100;
    end_E_search   = 1/100;
    % Find the position where the elongation surpasses..
    % 0.05 but is less than
    % 1%. E will be calculated between; 0.05% and 1% elongation.
    start_E = find(virg(:,6,j) >= begin_E_search,1, 'first');
    finish_E = find(virg(:,6,j) >= end_E_search,1, 'first')-1;

    % Calculate first order fit
    polynom = polyfit(virg(start_E:finish_E,6,j),...
    virg(start_E:finish_E,9,j),1);
    % save E per dog bone
    virg(3,10,j) = polynom(1);

    % number of used data points
    N_used      = length((virg(start_E:finish_E,6,j)));
    virg(4,10,j) = N_used;
    check_me    = polynom(1)*virg(start_E:finish_E,6,j)...
    +polynom(2);
    error(1:N_used,j) = ((virg(start_E:finish_E,9,j)... -
check_me)./(virg(start_E:finish_E,9,j)));
    % Data was bad at beginning. Thus if data is bad we look for the next
    % point till error is less than 5%
    while max(error(1,j)) >= 0.05
        % make error collumn empty again
        error(1:20,j) = nan(20,1);
        start_E      = start_E+1;
        polynom      =polyfit(virg(start_E:finish_E,6,j)..
, virg(start_E:finish_E,9,j),1);
        virg(3,10,j) = polynom(1);
        % number of used data points
        N_used      = length((virg(start_E:finish_E,6,j)));
        virg(4,10,j) = N_used;

```



```

        check_me      = polynom(1)*virg(start_E:finish_E,6,j)...
        +polynom(2);
        error(1:N_used,j)= ((virg(start_E:finish_E,9,j) -
check_me)./(virg(start_E:finish_E,9,j)));
    end

% Make different plots for checking if processing was correct.
% X = transpose(0:0.01:1);
% figure(4)
% hold on
% grid on
% plot(virg(:,6,j),virg(:,9,j))
% plot(virg(start_E:finish_E,6,j),polynom(1)*...
virg(start_E:finish_E,6,j)+polynom(2))
% plot(X,(virg(3,10,j)*X+polynom(2)))
% plot(virg(:,6,j),virg(:,9,j),'o')
end

% Calculate mean and plot.
final_mean = min(finals);
mean_virg = mean(virg(1:final_mean, :, :), 3);
std_virg = std(virg(1:final_mean, :, :), 0, 3);
% shift the mean such that it starts at 0
if mean_virg(1,9) < 0
    mean_virg(:,9) = mean_virg(:,9) - mean_virg(1,9);
    mean_virg(:,6) = mean_virg(:,6) - mean_virg(1,6);
end

plot(mean_virg(:,6),mean_virg(:,9),'LineWidth',2)
legend('1','2','3','4','5','6','mean')
hold off
% make separate vector for easy plotting at end.
% average and std sigma max
avg_sigma_m(1,2) = mean_virg(1,10);
std_sigma_m(1,2) = std_virg(1,10);
% average max strain
avg_strain_m(1,2)= mean_virg(2,10);
std_strain_m(1,2)= std_virg(2,10);
% average and std E
avg_E(1,2) = mean_virg(3,10);
std_E(1,2) = std_virg(3,10);

```


B

Linear fit of the material properties with a 95% prediction interval

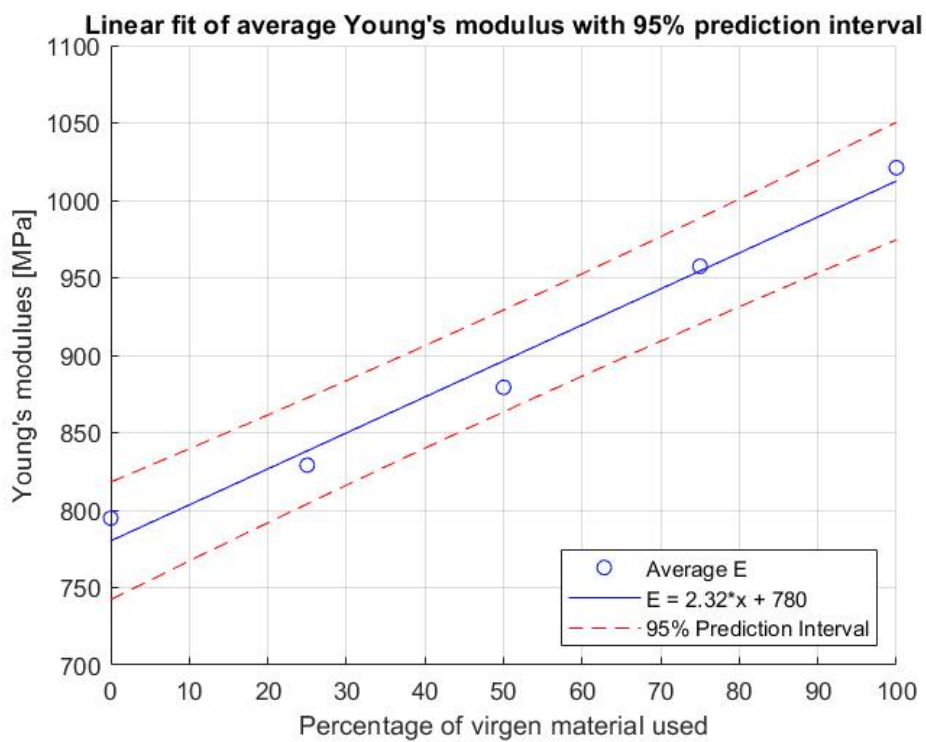


Figure B.1: Linear fit of the Young's modulus with 95% prediction interval.

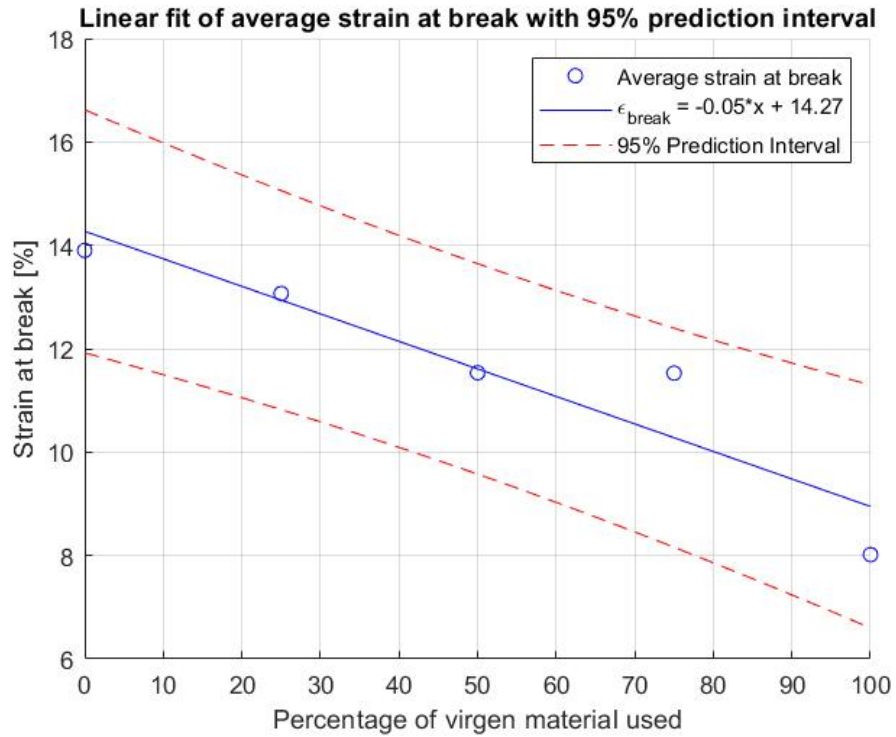


Figure B.2: Linear fit of the strain at break with 95% prediction interval.

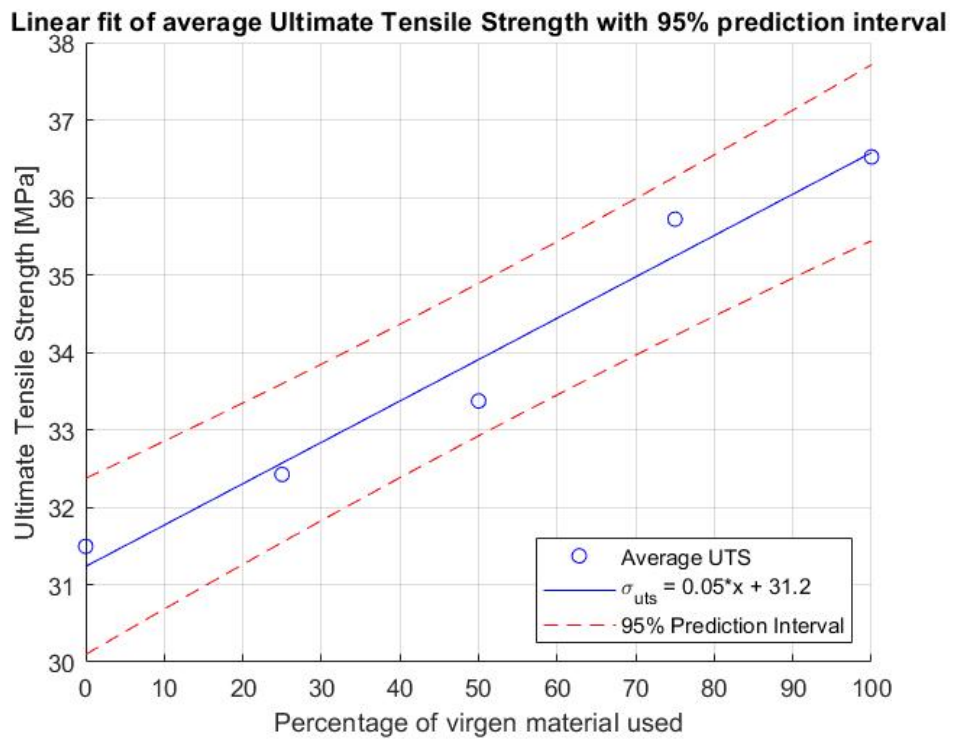


Figure B.3: Linear fit of the UTS at break with 95% prediction interval.

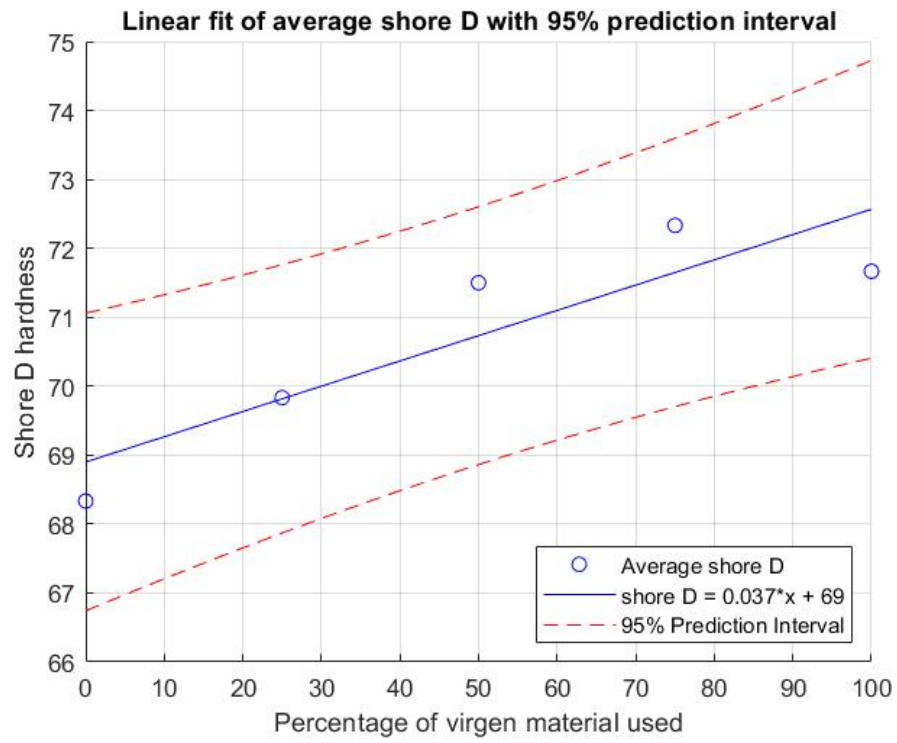
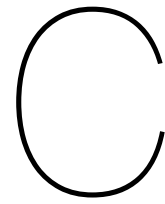


Figure B.4: Linear fit of the shore D hardness with 95% prediction interval



Matlab code: Temperature profile

Contents

- IR data processing Affordable filter
- Combination plot file

IR data processing Affordable filter

Daan van der Heiden 10-11-2021 close all;

```
clear

% number of frames
time = 00:3:36;
% makes space
L1 = nan(13,300);
L2 = nan(13,300);
L3 = nan(13,100);
L4 = nan(13,100);
L5 = nan(13,100);
L6 = nan(13,100);

for i = 1 : length(time)
    % make name vector
    filename{i,1} = strcat('Aff_t',num2str(time(i)),'.csv');

    %import lines. seperated by ,
    L1_i = readmatrix(filename{i,1},'Delimiter',' ','Range','B5:ZZ5');
    L2_i = readmatrix(filename{i,1},'Delimiter',' ','Range','B9:ZZ9');
    L3_i = readmatrix(filename{i,1},'Delimiter',' ','Range','B13:ZZ13');
    L4_i = readmatrix(filename{i,1},'Delimiter',' ','Range','B17:ZZ17');
    L5_i = readmatrix(filename{i,1},'Delimiter',' ','Range','B21:ZZ21');
    L6_i = readmatrix(filename{i,1},'Delimiter',' ','Range','B25:ZZ25');
    % place at righ place in grand matrix
    L1(i,1:length(L1_i)) = L1_i(:, :);
    L2(i,1:length(L2_i)) = L2_i(:, :);
    L3(i,1:length(L3_i)) = L3_i(:, :);
    L4(i,1:length(L4_i)) = L4_i(:, :);
    L5(i,1:length(L5_i)) = L5_i(:, :);
    L6(i,1:length(L6_i)) = L6_i(:, :);
end
```

```

plate_left    = readmatrix("notes_test_aff.xlsx","Range",'B3:B15');
plate_right   = readmatrix("notes_test_aff.xlsx","Range",'C3:C15');
ambient_temp  = readmatrix("notes_test_aff.xlsx","Range",'D3:D15');

% right line
max_L1 = max(L1, [], 2);
min_L1 = min(L1, [], 2, 'omitnan');
mean_L1 = mean(L1, 2, 'omitnan');
std_L1  = std(L1, [], 2, "omitnan");

% left line
max_L2 = max(L2, [], 2);
min_L2 = min(L2, [], 2, 'omitnan');
mean_L2 = mean(L2, 2, 'omitnan');
std_L2  = std(L2, [], 2, "omitnan");

% middle lines
% place middle lines in one array
mid_filter(:, :, 1) = L3;
mid_filter(:, :, 2) = L4;
mid_filter(:, :, 3) = L5;
mid_filter(:, :, 4) = L6;

% calculate mean max min and find location
mean_mid_filter = mean(mid_filter, [2 3], 'omitnan');
[max_mid_filter, I_max] = max(mid_filter, [], [2 3], "omitnan", "linear");
[min_mid_filter, I_min] = min(mid_filter, [], [2 3], "omitnan", "linear");
std_mid_filter         = std(mid_filter, [], [2 3], "omitnan");

% indices max
[row_max, col_max, page_max] = ind2sub(size(mid_filter), I_max);
[row_min, col_min, page_min] = ind2sub(size(mid_filter), I_min);

% check if max/min is found in the correct position.
indx_min = num2cell([row_min, col_min, page_min]);

for i = 1:13
    min_check(i, :) = mid_filter(indx_min{i, :});
end

check = min_mid_filter - min_check;

% Boxplots
% place in different matrix for boxplots format
mid_filtert = L3;
mid_filtert(:, 101:200) = L4;
mid_filtert(:, 201:300) = L5;
mid_filtert(:, 301:400) = L6;
% reshape to boxplot format
mid_filtert = mid_filtert';
mid_filtert = mid_filtert(:);
% also reshape for time
time_filter = repelem(time, (length(mid_filtert)/length(time)));

```

```

L2t = L2(:,1:end-1)';
L2t = L2t(:);

L1t = L1(:,1:end-1)';
L1t = L1t(:);
time_sides = repelem(time, (length(L1t)/length(time)));

figure(3)
grid on
hold on
plot(time,mean_L1,'Color','#0072BD')
plot(time,mean_L2,'Color','#D95319')
plot(time,mean_mid_filter,'Color','#A2142F')
plot(time,ambient_temp,'Color','#EDB120')
plot([24 24],[0 250],'Color','k','LineWidth',1.2)

boxchart(time_sides,L1t,'BoxFaceColor','#0072BD','MarkerColor','#0072BD')
boxchart(time_sides,L2t,'BoxFaceColor','#D95319','MarkerColor','#D95319')
box_aff = boxchart(time_filter,mid_filtert,'BoxFaceColor','#A2142F', ...
    'MarkerColor','#A2142F');
title('Temperature mean and boxplots of Affordable filter over time')
legend('Right plate','Left plate','Middle filter', ...
    'Ambient temperature','Start cooldowncycle')
xlabel('Time [min]')
ylabel('Temperature [C]')
xticks(time)
yticks([0:25:250])
xlim([0 37])
hold off
% master plot file
clear;

```

Combination plot file

```

run(['D:\Desktop D\Scholla\Master\Thesis\Heatmapping\Thesis\' ...
    'Test_2_Cycle_time\Gif\line_data\CT_data_process.m'])
run(['D:\Desktop D\Scholla\Master\Thesis\Heatmapping\Thesis\' ...
    'Test_5-Compatible\GIF\line_data\Comp_data_process.m'])
run(['D:\Desktop D\Scholla\Master\Thesis\Heatmapping\Thesis\' ...
    'Test_4_Affordable\GIF\line_data\aff_data_process.m'])
%load boxplots for each filter for final figure
load('box_comp.mat')
load('box_CT.mat')
load('box_aff.mat')

```

close all

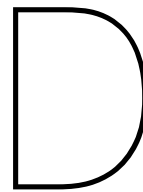
```

figure(4)
hold on
grid on
plot(time,mean_mid_CT,'Color','#77AC30')
plot(time,mean_mid_aff,'Color','#A2142F')
plot(time,mean_mid_comp,'Color','#7E2F8E')
plot([24 24],[0 150],'Color','k','LineWidth',1.2)

boxchart(time_filter,box_CT.YData,'BoxFaceColor', ...

```

```
'#77AC30','MarkerColor','#77AC30')
boxchart(time_filter,box_aff.YData,'BoxFaceColor', ...
'#A2142F','MarkerColor','#A2142F')
boxchart(time_filter,box_comp.YData,'BoxFaceColor', ...
'#7E2F8E','MarkerColor','#7E2F8E')
title('Temperature mean and boxplots of filters over time')
legend('Cycle Time filter','Affordable filter','Compatible filter' ...
,'Start cooldowncycle')
xlabel('Time [min]')
yticks([0:25:150])
xticks(time)
xlim([0 37])
ylabel('Temperature [C]')
```



FEM analyses: stress strain figures

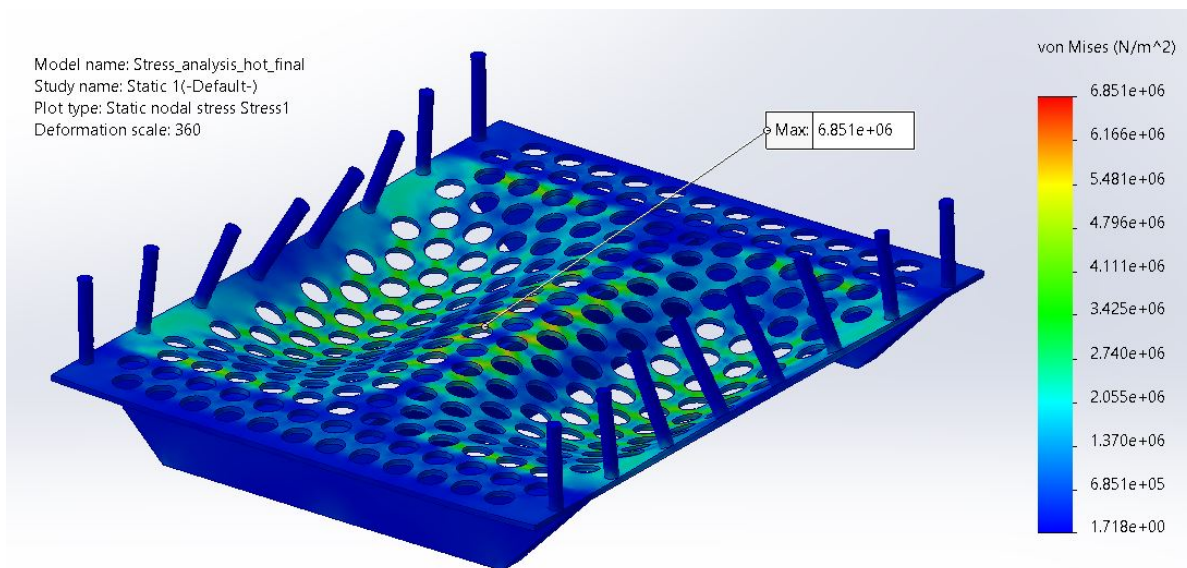


Figure D.1: Stress and deformation profile on the Minimize Cycle Time filter from the FEM analyses in Solidworks.

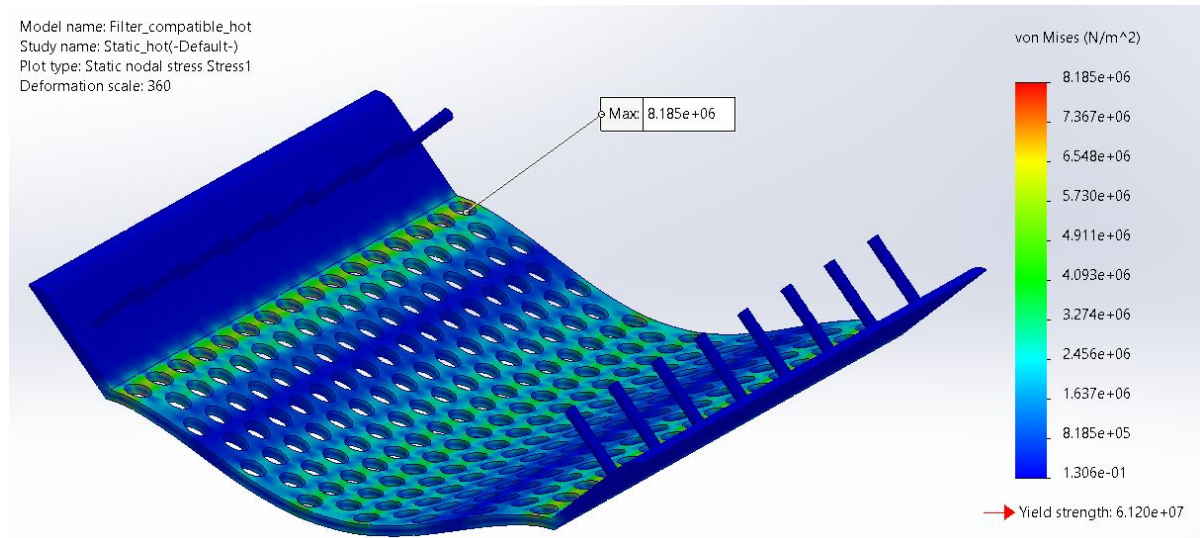


Figure D.2: Stress and deformation profile on the Compatible filter from the FEM analyses in Solidworks.

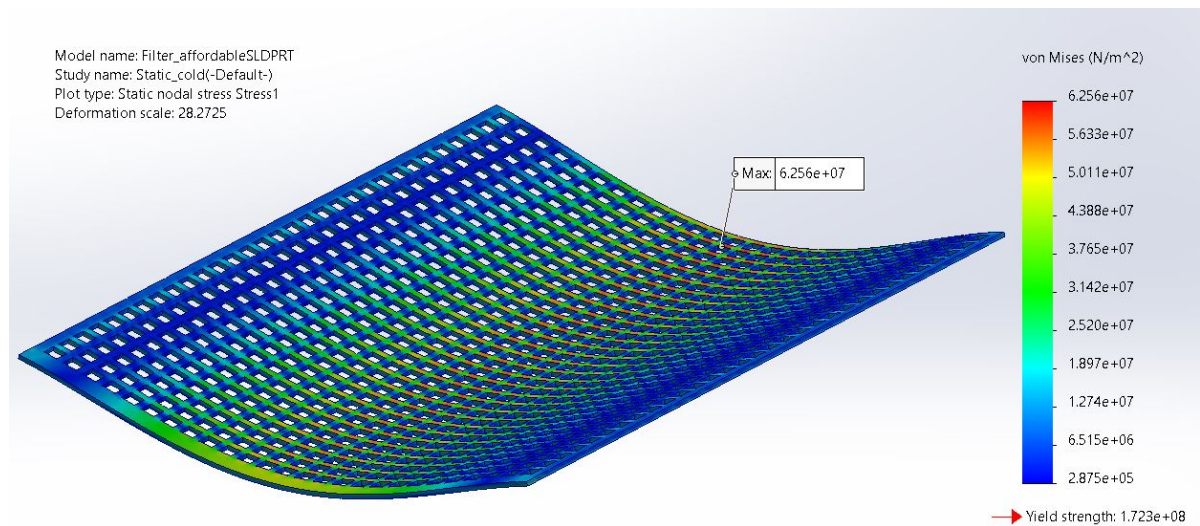


Figure D.3: Stress and deformation profile on the affordable filter from the FEM analyses in Solidworks.

Bibliography

- Assemu, D. M., Tafere, T. E., Gelaw, Y. M., & Bantie, G. M. (2020). Healthcare waste management practice and associated factors among private and public hospitals of bahir dar city administration. <https://doi.org/10.1155/2020/7837564>
- Aurrekoetxea, J., Sarrionandia, M. A., Urrutibeascoa, I., & Maspoch, M. L. (2001). Effects of recycling on the microstructure and the mechanical properties of isotactic polypropylene. *Journal of Materials Science*, *36*, 2607–2613. <https://doi.org/10.1023/A:1017983907260>
- Babu, M. A., Dalenberg, A. K., Goodsell, G., Holloway, A. B., Belau, M. M., & Link, M. J. (2019). Greening the operating room: Results of a scalable initiative to reduce waste and recover supply costs. *Clinical Neurosurgery*, *85*, 432–437. <https://doi.org/10.1093/neuros/nyy275>
- Bliss, L. M., Ecklund, J. M., & Riley, J. B. (1995). Recycling of renewable resources in extracorporeal circulation technology [oud 1995 gaat over percentage plastic in ziekhuisafval is inmiddels helemaal anders.]. *Journal of Extra-Corporeal Technology*, *27*, 81–84.
- Bokhoree, C. (2014). Assessment of environmental and health risks associated with the management of medical waste in mauritius. *APCBEE Procedia*, *9*, 36–41. <https://doi.org/10.1016/j.apcbee.2014.01.007>
- C, P. A. bibinitperiod. (2020). *Polypropylene material safety data sheet*. https://www.acplasticsinc.com/techsheets/Polypropylene_MSDS.pdf
- Chudasama, R. (2014). Awareness and practice of biomedical waste management among different health care personnel at tertiary care centre, rajkot, india. *Online Journal of Health and Allied Sciences*, *13*.
- da Costa, H. M., Ramos, V. D., & de Oliveira, M. G. (2007). Degradation of polypropylene (pp) during multiple extrusions: Thermal analysis, mechanical properties and analysis of variance. *Polymer Testing*, *26*, 676–684. <https://doi.org/10.1016/j.polymeresting.2007.04.003>
- Eckelman, M. J., & Sherman, J. (2016). Environmental impacts of the u.s. health care system and effects on public health. <https://doi.org/10.1371/journal.pone.0157014>
- Gabriel, D. S., & Tiana, A. N. (2020). Mechanical properties improvement of recycled polypropylene with material value conservation schemes using virgin plastic blends. *Materials Science Forum*, *1015 MSF*, 76–81. <https://doi.org/10.4028/www.scientific.net/MSF.1015.76>
- Ghajar, A., & Yunus A. Cengel, D. (2014). *Heat and mass transfer: Fundamentals and applications*. McGraw-Hill Education. <https://books.google.nl/books?id=B89MnwEACAAJ>
- Ghodrat, M., Rashidi, M., & Samali, B. (2017). Life cycle assessments of incineration treatment for sharp medical waste. *Minerals, Metals and Materials Series*, 131–143. https://doi.org/10.1007/978-3-319-52192-3_14
- Goldberg, M. E., Vekeman, D., Torjman, M. C., Seltzer, J. L., & Kynes, T. (1996). Medical waste in the environment: Do anesthesia personnel have a role to play? *Journal of Clinical Anesthesia*, *8*, 475–479. [https://doi.org/10.1016/0952-8180\(96\)00127-4](https://doi.org/10.1016/0952-8180(96)00127-4)
- Haque, M. S., Uddin, S., Sayem, S. M., & Mohib, K. M. (2021). Coronavirus disease 2019 (covid-19) induced waste scenario: A short overview. *Journal of Environmental Chemical Engineering*, *9*, 104660. <https://doi.org/10.1016/j.jece.2020.104660>
- Hoegh-Guldberg, O. (2015). Plastic waste inputs from land into the ocean. *Science*, *347*, 768–770. <http://www.scopus.com/inward/record.url?eid=2-s2.0-84954204572&partnerID=40&md5=28a97ef4a4fdee6db9ef2fe507a1a02a>
- Hopkinson, J., Sa, D., Rowland, *, & Mag, P. (1888). *Xiv. magnetic and other physical properties of iron at a high temperature* [DIE VOOR JE TIM!].
- Hyie, K. M., Budin, S., Halidi, S. N., & Fohimi, N. A. (2020). Durability of repetitive polypropylene recycling: Challenge on securing the mechanical properties. *IOP Conference Series: Materials Science and Engineering*, *1003*. <https://doi.org/10.1088/1757-899X/1003/1/012127>

- Irianti, S. (2013). Current status and future challenges of healthcare waste management in Indonesia. *Current Status and Future Challenges of Healthcare Waste Management in Indonesia*, 23, 73–81. <https://doi.org/10.22435/mpk.v23i2.3129.73-81>
- Lee, R. J., & Mears, S. C. (2012). Reducing and recycling in joint arthroplasty. *Journal of Arthroplasty*, 27, 1757–1760. <https://doi.org/10.1016/j.arth.2012.04.020>
- Lehner, G. (2010). *Maxwell's equations*. https://doi.org/10.1007/978-3-540-76306-2_1
- Manga, V. E., Forton, O. T., Mofor, L. A., & Woodard, R. (2011). Health care waste management in Cameroon: A case study from the southwestern region. *Resources, Conservation and Recycling*, 57, 108–116. <https://doi.org/10.1016/j.resconrec.2011.10.002>
- McGain, F., Hendel, S. A., & STORY, D. A. (2009). *An audit of potentially recyclable waste from anaesthetic practice* (5).
- McGain, F., Jarosz, K. M., Nguyen, M. N. H. H., Bates, S., & O'Shea, C. J. (2015). Auditing operating room recycling: A management case report. *A & A case reports*, 5, 47–50. <https://doi.org/10.1213/XAA.0000000000000097>
- Penn, E., S., Y., & J., W. (2012). Reducing disposable equipment waste for tonsillectomy and adenotonsillectomy cases. *Otolaryngology - Head and Neck Surgery (United States)*, 147, 615–618. <https://doi.org/10.1177/0194599812450681>
- Pinto, V., Joshi, S., Velankar, D., Mankar, M., Bakshi, H., & Nalgundwar, A. (2014). A comparative study of knowledge and attitudes regarding biomedical waste (BMW) management with a preliminary intervention in an academic hospital. *International Journal of Medicine and Public Health*, 4, 91. <https://doi.org/10.4103/2230-8598.127166>
- Pullishery, F., Panchmal, G., Siddique, S., & Abraham, A. (2016). Awareness, knowledge and practices on bio-medical waste management among health care professionals in Mangalore- a cross sectional study. *International Archives of Integrated Medicine*, 3, 29–35.
- Razali, S. S., & Ishak, M. B. (2010). Clinical waste handling and obstacles in Malaysia. *Journal of Urban and Environmental Engineering*, 4, 47–54. <https://doi.org/10.4090/juee.2010.v4n2.047054>
- Rigante, L., Moudrous, W., Vries, J. D., Grotenhuis, A. J., & Boogaarts, H. D. (2017). Operating room waste: Disposable supply utilization in neurointerventional procedures. <https://doi.org/10.1007/s00701-017-3366-y>
- Shum, P. L., Kok, H. K., Maingard, J., Schembri, M., Bañez, R. M. F., Damme, V. V., Barras, C., Slater, L. A., Chong, W., Chandra, R. V., Jhamb, A., Brooks, M., & Asadi, H. (2020). Environmental sustainability in neurointerventional procedures: A waste audit. *Journal of NeuroInterventional Surgery*, 12, 1053–1057. <https://doi.org/10.1136/neurintsurg-2020-016380>
- Silva, A. L. P., Prata, J. C., Walker, T. R., Duarte, A. C., Ouyang, W., Barcelò, D., & Rocha-Santos, T. (2021). Increased plastic pollution due to COVID-19 pandemic: Challenges and recommendations. *Chemical Engineering Journal*, 405, 126683. <https://doi.org/10.1016/j.cej.2020.126683>
- Southorn, T., Norrish, A. R., Gardner, K., & Baxandall, R. (2013). Reducing the carbon footprint of the operating theatre: A multicentre quality improvement report. *Journal of Perioperative Practice*, 23, 144–146. <https://doi.org/10.1177/175045891302300605>
- Strategists, G. (2019). Een stuur voor de transitie naar duurzame gezondheidszorg kwantificering van de CO₂-uitstoot.
- Su, M. N., & Young, B. (2019). Material properties of normal and high strength aluminium alloys at elevated temperatures. *Thin-Walled Structures*, 137, 463–471. <https://doi.org/10.1016/j.tws.2019.01.012>
- Sutrisno, H., & Meilasari, F. (2020). Review: Medical waste management for COVID-19. *Jurnal Kesehatan Lingkungan*, 12, 104. <https://doi.org/10.20473/jkl.v12i1si.2020.104-120>
- van der Heiden, D. (2020). Internship report.
- van Straten, B., van der Heiden, D., Robertson, P., Riekwel, C., Jansen, F., van der Elst, M., & Horeman, T. (2021). Surgical waste reprocessing: Injection molding using recycled blue wrapping paper from the operating room. *Journal of Cleaner Production*, 322. <https://doi.org/10.1016/j.jclepro.2021.129121>
- Voudrias, E. A. (2018). Healthcare waste management from the point of view of circular economy. *Waste Management*, 75, 1–2. <https://doi.org/https://doi.org/10.1016/j.wasman.2018.04.020>
- White, S. M., Sanghera, P., & Chakladar, A. (2010). Estimate of the carbon footprint of the US health care sector. *Age and Ageing*, 39, 650–653. <https://doi.org/10.1093/ageing/afq078>

- Wyssusek, K. H., Foong, W. M., Steel, C., & Gillespie, B. M. (2016). The gold in garbage: Implementing a waste segregation and recycling initiative. *AORN Journal*, *103*, 316.e1–316.e8. <https://doi.org/10.1016/j.aorn.2016.01.014>
- Yong, Z., Gang, X., Guanxing, W., Tao, Z., & Dawei, J. (2009). Medical waste management in china: A case study of nanjing. *Waste Management*, *29*, 1376–1382. <https://doi.org/10.1016/j.wasman.2008.10.023>
- Zhang, H. J., Zhang, Y. H., Wang, Y., Yang, Y. H., Zhang, J., Wang, Y. L., & Wang, J. L. (2013). Investigation of medical waste management in gansu province, china. *Waste Management and Research*, *31*, 655–659. <https://doi.org/10.1177/0734242X13482161>